MASTER'S DEGREE THESIS

Master of Science in Advanced Mathematics and Mathematical Engineering

Title: Modelling attentional biases in bistable perception

Author: Marina Vilardell Barnosell

Advisors: Antoni Guillamon

Department: Universitat Politècnica de Catalunya - FME

Academic year: 2018 - 2019

UNIVERSITAT POLITÈCNICA DE CATALUNYA
BARCELONATECH
Facultat de Matemàtiques i Estadística

Universitat Politècnica de Catalunya
Facultat de Matemàtiques i Estadística

Master in Advanced Mathematics and Mathematical Engineering

Master's thesis

Modelling attentional biases in bistable perception

Marina Vilardell Barnosell

Supervised by Antoni Guillamon

June, 2019

I would like to thank my supervisor, Toni Guillamon, for his help and advise throughout the study and completion of the thesis.

And to my family, for their support and continuous encouragement.

Abstract

Binocular rivalry is a type of bistable perception phenomena that arises when the eyes are unable to combine ambiguous stimuli into a unique image. It promotes a competition process between the visual interpretations received, in the form of oscillations between dominant and suppressed states. Recent research has suggested that, in binocular rivalry, visual attention is an external factor that influences the dynamics behind the perception of stimuli. This thesis will discuss the effect of attention in an extended version of Curtu et al. (2008)'s binocular rivalry model by analysing the way in which recurrent excitatory inputs applied on neurons change how stimuli are perceived. By analysing the relationship between a self-recurrent excitation term, the input strength and the inhibition parameter through bifurcation and two-parameter diagrams, we concluded that attention has a direct effect on frequency dynamics; promoting faster oscillatory regimes as well as the achievement of Winner-Take-All behaviours through release and escape mechanisms.

Keywords

Binocular rivalry, attention, release, escape, oscillatory dynamics

Contents

1 Introduction **3**

2 General overview on current models illustrating bistable perception **5**
2.1 Background on bistable perception and visual attention 5
2.2 A Binocular Rivalry rate model for a network of Hodgkin-Huxley-like neurons 6
2.3 A simplified Binocular Rivalry model: Curtu et al. (2008) 7
2.4 Noise-attractor models: Moreno-Bote, Rinzel and Rubin (2007) 8
2.5 Visual attention in Binocular Rivalry 9

3 Analysis of an existing model of bistable perception: Curtu et al. (2008) **11**
3.1 Equilibria and bifurcations 11
3.1.1 Stability analysis of p^*: Preliminary analysis 13
3.1.2 Stability analysis of p^*: Dynamics illustrating a Hopf bifurcation 17
3.2 An introduction to release, escape and Winner-Take-All mechanisms 19
3.2.1 A toy example: Heaviside function 19
3.3 Bifurcation diagrams and Levelt's propositions 32

4 Visual attention as a recurrent excitatory input **36**
4.1 The extended model 36
4.2 Diagrams and results obtained 37

5 Conclusion **43**

A Li et al. (2017)'s attention model **46**
A.1 General overview of the model 46
A.2 Results obtained 50

B An introduction to the slow variables' manifold for the sigmoid gain function **51**

C XPP codes **55**
C.1 Curtu (2008)'s model 55
C.2 Curtu (2008)'s model with excitatory recurrence 56
C.3 Li et al. (2017)'s attention model 57

1. Introduction

The images that we view can differ depending on how visual stimuli are percieved by the eyes. If visual inputs received are ambiguous or comparatively different from each other, the eyes will be unable to fuse them into one single image, promoting the appearance of perceptual alternations [5, 6, 12]. Bistable perception is a neuronal phenomena present in situations where perceived stimuli lead to ambiguous interpretations of an image [1, 2]. This would cause continuous alternations between stimuli perceived and therefore, individuals would only experience separate snapshots of the real image [5, 6, 12, 13].

Bistable perception encovers different perception mechanisms; one of them is Binocular Rivalry which is characterised by promoting a competition process on contrasting stimuli [1, 2, 7, 10, 11]. Figure 1 presents a schematic description of Binocular Rivalry. Briefly, this particular phenomena arises when there exists a bistability process between stimuli regulated by suppression and adaptation mechanisms, leading to continuous alternations on neuronal dynamics [5, 6, 12, 13].

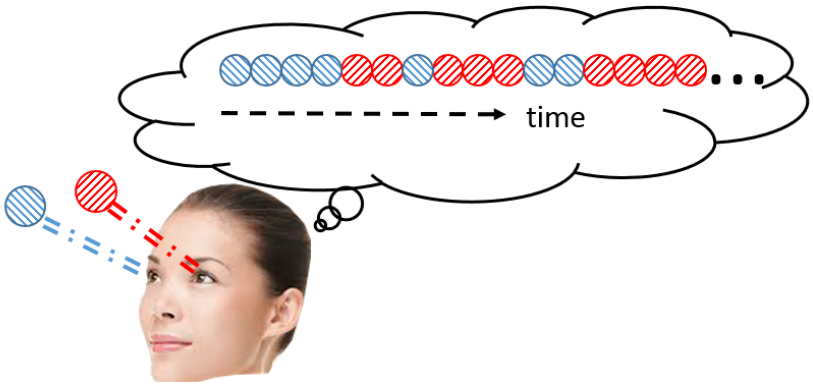

Figure 1: Schematic description of binocular rivalry.

Moreover, in recent years, there has been an interest in understanding the effect of external and internal factors such as visual attention in binocular rivalry processes. It seems that attention could be a necessary factor to induce alternations and changes on the dynamics between different stimuli perceived - see [6]. In addition, in 2017 Li et al. went deeper into the topic and suggested that specific groups of neurons were responsible for modelling different neuronal mechanisms. In their research, the authors derived a model formed by a system of eighteen equations where attention contributions were regulated by a pool of attention neurons [9].

The aim of the thesis is to research and discuss the effect of visual attention in the way neurons perceive and interact with stimuli that induce binocular rivalry. For that, our first and initial objective was to offer an introductory background that led to the replication and extension of the results found by Li et al. (2017) in their research paper. However, due to the level of detail that characterizes the research and the qualitative gap between Li et al.'s model and past research on the topic, we found ourselves unable to correctly reproduce the main results presented in the paper. For that reason, and after correspondence with some of the authors of the study, we realised that attention could also be considered as a self-excitatory recurrence applied on neurons, giving us the opportunity to apply the new hypothesis in the binocular rivalry model

proposed by Curtu et al. in 2008 [5]. Nevertheless, as we consider Li et al.'s article to be an interesting and innovating research on the topic, we have included a thorough background of the model in Appendix A with the corresponding XPP code included in Appendix C.

Overall, the thesis is structured such that in Chapter 2 an introductory background to bistable phenomena and binocular rivalry is presented, giving an overview on some models that were devised in recent years. It then follows with a thorough analysis of the model of Curtu et al. in Chapter 3, replicating the results presented in the article - see [5]. Finally, the thesis concludes with Chapter 4 where it analyses and discusses the effect and influence of visual attention, represented by the addition of a self-excitatory parameter D on an extension of Curtu et al.'s model.

2. General overview on current models illustrating bistable perception

2.1 Background on bistable perception and visual attention

In some situations the eyes may perceive stimuli that are ambiguous or have different interpretations that are not comparable to each other. In these cases, percepts - or stimuli perceived - start to regularly alternate between each other, also motivating an alternation of the images viewed [5, 6, 12]. **Bistable perception** is a phenomena known in neuroscience that occurs when two images perceived are too ambiguous or open to different interpretations. In these situations, the whole image will not be entirely viewed, and so the individual will only experience different stimuli separately [1, 2]. In other words, this phenomena will cause spontaneous and continuous switches between the possible percepts, allowing only one to be seen at each time [5, 6, 12, 13]. The term Bistable Perception includes different multistable perceptual experiences such as ambiguous images or the Necker Cube, both shown in Figure 2.

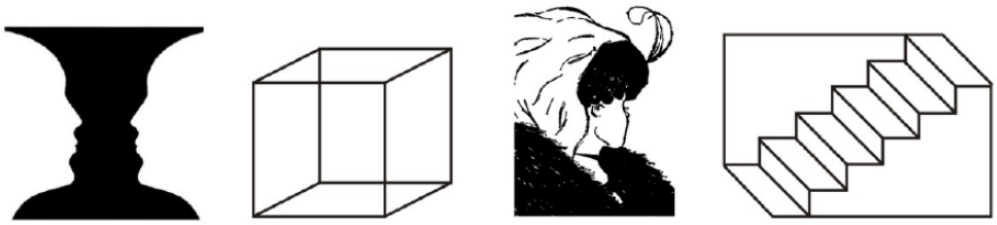

Figure 2: Examples of stimuli that can cause Bistable Perception

Moreover, the way in which eyes perceive different stimuli differs depending on how many eyes are actively viewing an image at a particular moment of time. **Monocular vision** is a term used to refer the cases in which individuals only see through one of the eyes. In contrast, **binocular vision** is normally used to describe situations where both eyes are being actively used to look at a certain object or space. This sometimes leads to an overlapping between the snapshots of the picture that is being viewed by each eye [2]. Similarly, there also exist two types of neurons that receive information from the eyes and send it to the brain. We use the term **monocular** to characterize the neurons that only receive stimuli from one eye, whereas, **binocular neurons** are sensible to information from both eyes [2].

One of the forms of bistable perception is **binocular rivalry**, a neural process in which both eyes receive different visual inputs that unsuccessfully attempt to combine into one single image. Due to this overlapping, the two stimuli start to compete for dominance, causing a periodic change on the general dynamics of the system [2, 7, 10, 11]. Percepts will then become regulated by means of some suppression and adaptation mechanisms that will eventually control when each image is dominant and therefore, viewed [7, 11]. Note that in neuroscience, as well as in population dynamics, competition is defined as the biological process where one species is negatively affected by another [5]. In addition, it is important to remark on the difference between bistable perception and binocular rivalry. Not all bistable perceptual mechanisms eventually drive a competition process between two percepts [6].

On the other hand, research has also shown that there exists specific criteria for analysing and comprehending neuron models and their dynamics. In particular, in 1965 Levelt developed four different propositions that were used to analyse the behaviour of neuron models and relate their oscillatory dynamics with the variation of parameters such as the external input received, I [3]. The propositions are stated as follows:

(I) Increasing the strength of stimuli for one eye will increase the dominance of that eye's perception [3].

(II) Increasing the strength of one eye's percept will not affect its dominance duration. However, it will reduce the predominance time of the opposite eye's perception [3].

(III) Increasing the percept's strength of one of the eyes directly increases the switching rate between percepts - or rivalry rate [3, 7].

(IV) The dominance time of different percepts will decrease if the percepts' strength are simultaneously increased for both eyes [3].

The above propositions will be cited and used throughout the chapters of this thesis to analyse and comprehend the neural behaviour and possible dynamics of different binocular rivalry models. On the following sections, current models that illustrate binocular rivalry phenomena will be briefly discussed, altogether with some of the results and conclusions obtained. In addition, from this section onwards, the word *population* will be used when referring to different groups of spiking neurons that receive different stimuli or perceptual inputs.

2.2 A Binocular Rivalry rate model for a network of Hodgkin-Huxley-like neurons

Laing and Chow [8] understood binocular rivalry as a biophysiological process where competition occurred between a pair of spiking neurons. Their research was designed around the hypothesis that each stimulus was linked to some neurons that were only activated when the corresponding percept was dominant. The research used both inhibitory and excitatory Hodgkin-Huxley-type neurons to model their orientation and coupling. Furthermore, Laing and Chow illustrated the effect of external factors such as adaptation (i.e. depression on the alternation rate), dominance time and neuron populations' strength, by only focusing on neurons whose activity increased when their corresponding percept was dominant [8]. The authors concluded that neurons that had a preferred orientation only connected to others of a similar type by noting that neurons that belonged to different percepts were unable to sustain their activity at the same time, and therefore fuse into one single image [8].

$$
\begin{cases}
\dfrac{du_1}{dt} = -u_1 + f(\alpha u_1 g_1 - \beta u_2 g_2 - a_1 + I_1) & (1)\\
\dfrac{du_2}{dt} = -u_2 + f(\alpha u_2 g_2 - \beta u_1 g_1 - a_2 + I_2) & (2)\\
\tau_a \dfrac{da_1}{dt} = -a_1 + \phi_a f(\alpha u_1 g_1 - \beta u_2 g_2 - a_1 + I_1) & (3)\\
\tau_a \dfrac{da_2}{dt} = -a_2 + \phi_a f(\alpha u_2 g_2 - \beta u_1 g_1 - a_2 + I_2) & (4)\\
\tau_d \dfrac{dg_1}{dt} = 1 - g_1 - g_1 \phi_d f(\alpha u_1 g_1 - \beta u_2 g_2 - a_1 + I_1) & (5)\\
\tau_d \dfrac{dg_2}{dt} = 1 - g_2 - g_2 \phi_d f(\alpha u_2 g_2 - \beta u_1 g_1 - a_2 + I_2) & (6)
\end{cases}
$$

In Laing and Chow's model, $u_{1,2}$ represent the spiking activity of each type of neuron, $a_{1,2}$ illustrate the effect of adaptation and $g_{1,2}$ model the effect of synaptic depression. On the other hand, τ_a and τ_d are time constants respectively associated to frequency adaptation processes and depression. Finally, the function f illustrates the input-output function represented by a Heaviside-step function [8]. Note that equations (1), (3), (5) model the behaviour of excitatory neurons whereas (2), (4) and (6) characterise inhibitory neurons.

Laing and Chow's research concluded that the model's design nicely represented the behaviour of binocular rivalry processes. Their results supported *Levelt's second proposition* by showing that the dominance time of a percept was directly influenced by its strength. Nevertheless, they also suggested that other external factors such as ambiguity on percepts, noise and contrast between two stimuli could affect alternation rates and dominance times.

2.3 A simplified Binocular Rivalry model: Curtu et al. (2008)

Curtu et al. [5] designed a model of binocular rivalry that illustrated the effect of competition between two eyes' stimuli. In other words, the model suggested that each population respectively inhibited the other only when they were dominant [5]. In addition, external factors such as frequency adaptation (representing cellular fatigue and synaptic depression) were considered to influence the behaviour between two populations of spiking neurons [5].

Curtu et al.'s model considers four equations and two main variables that illustrate the interaction between two populations that regulate each other through reciprocal inhibition and slow adaptive processes. Note that in the research both stimuli were considered to have equal strength [5].

$$
\begin{cases}
\dfrac{du_1}{dt} = -u_1 + S(I - \beta u_2 - g a_1)\\
\dfrac{du_2}{dt} = -u_2 + S(I - \beta u_1 - g a_2)\\
\tau \dfrac{da_1}{dt} = -a_1 + u_1\\
\tau \dfrac{da_2}{dt} = -a_2 + u_2
\end{cases}
$$

Similarly to Laing and Chow's model, $u_{1,2}$ and $a_{1,2}$ are the main variables of the model which respectively measure the firing rate of the different populations of neurons and the fatigue (or adaptive behaviour) that affect the dominance of each of the stimulus [5]. Moreover, the following parameters are also used in the model to illustrate the external factors considered.

- β and g respectively model the inhibition strength and frequency adaptation of each population. It is important to remark that, as previously discussed, adaptation is modelled as an intrinsic process linked to each stimulus, but inhibition is thought to affect only the competitor.

- τ is an associated timescale that regulates the evolution of the adaptive variables $a_{1,2}$. τ will take large values to balance the difference in time evolution between $u_{1,2}$ and $a_{1,2}$.

- I models the intensity of the percept that is being perceived, whereas $S(I - \beta u_2 - g a_1)$ represents the input-output function of this model.

This model will be analysed and discussed in more detail in Chapter 3, following this introductory background, to illustrate the possible dynamics that can arise on competing neuron populations.

2.4 Noise-attractor models: Moreno-Bote, Rinzel and Rubin (2007)

Moreno-Bote, Rinzel and Rubin worked with populations of excitatory and inhibitory neurons in order to study the behaviour and the effect that factors such as noise had in inducing alternations in binocular rivalry contexts [12]. We define *noise* as the fluctuations that occur within the spiking activity of neurons. Research suggests that noise can be caused by external and internal factors such as the eyes' blinking, directly affecting a percept's alternation rate [12]. However, specific factors that can cause spiking neurons to oscillate are still being researched.

The effect of noise in the strength and dominance of a stimulus was analysed by varying the strength of the percept and the external inputs that each population of neurons was receiving. The aim was to see whether this particular factor was one of the main causes of alternation between percepts [12]. The authors derived two models to illustrate the above arguments, considering noise as the only factor that induced alternation processes between percepts [12]. Figure 3 shows that both models consider an external subpopulation of inhibitory neurons to have an effect on the overall behaviour of the system, yet at the same time both populations of spiking neurons also have inhibitory effects on the competitor.

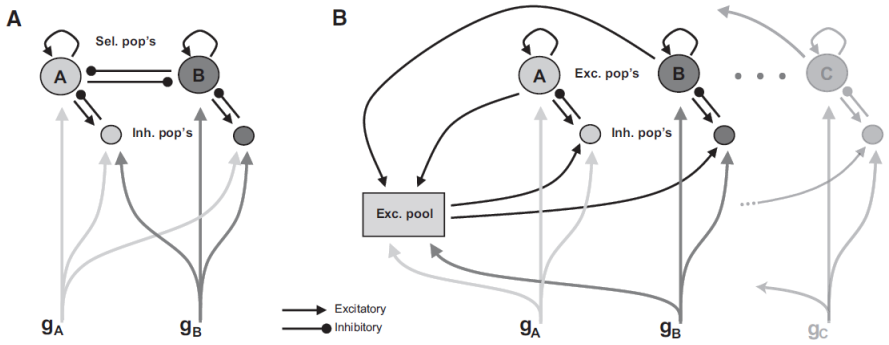

Figure 3: Two types of noise-attractor models derived by Moreno-Bote, Rinzel and Rubin in 2007 [12, p. 1129]

To conclude, findings suggest that the strength of percepts, and therefore corresponding inhibitory effect over a stimulus, is influenced by the external input received by inhibitory neurons [7, 12]. This result can be directly related with Levelt's propositions II and IV which illustrate the effect of dominance time over the strength of a stimulus [3].

2.5 Visual attention in Binocular Rivalry

The chapter will finish by introducing visual attention in the context of Binocular Rivalry. *Attention* is defined as a neuronal mechanism that selectively chooses specific percepts or stimuli among others [6]. It is important to remark the implications that visual attention can have in the perception of what we see. For instance, two people in the same room could have different perceptions of a scene if attention was only selecting parts of the images or stimuli that individuals have in front of them [6]. However, it is still undefined which specific role visual attention has in binocular rivalry processes. As it has been previously introduced, there are still questions unanswered regarding the effect of visual attention in bistable perception. For example, researchers are unsure on whether attention becomes key on influencing the alternating behaviours on percepts, or the role that it acquires over choosing the dominant percept [6].

Researchers differentiate between two types of attention processes that are thought to influence different neural behaviours: *partial attention* and *complete inattention*. The difference between both terms lies on the effect that they may have on bistable stimuli [6, 9]. Complete inattention occurs when alternations and inhibition between populations of neurons stop, allowing both stimuli to fuse into one single percept [6]. On the other hand, findings suggest that partial attention is characterised by slowing down the effect of inhibition and alternating rates [6].

One of the first models that considered an attention component within a system that represented a binocular rivalry process was Wilson's in 2003 [14]. The model studied the influence of orthogonal gratings in neuronal behaviour. Orthogonal gratings is a term that refers to the situation in which each eye is assigned to a different pattern, either vertical or horizontal [14]. Research showed that gratings were not stable and therefore, dominance switched between both eyes' stimuli promoting a rivalry behaviour. In his research article, Wilson (2003), explored the possible influence of attention as an external factor in a binocular rivalry context [14].

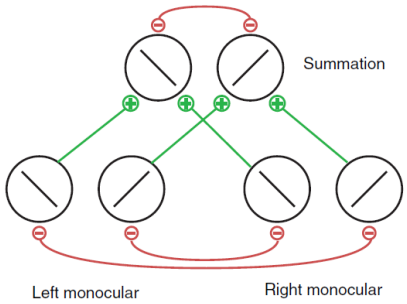

Figure 4: Wilson's model (2003) - figure quoted from [9]

Wilson's model considered three populations of neurons; one binocular and two of them monocular which belonged to the left and right eye respectively [14]. Each population had two neurons with a given orientation that illustrated vertical and horizontal gratings. The model was structured in two-stages, in which binocular neurons were placed in the second stage and received external input from monocular neurons [14].

On the other hand, Dieter et al.'s research focused on understanding how the competitiveness between percepts and their dominance time were influenced by visual attention [6]. Dieter et al. questioned themselves on whether percepts would stop alternating if a subject was not paying attention to the inputs received [6]. Findings show that inhibition of the percepts is directly influenced by visual attention, as the strength of the inhibitory factor is reduced considerably if the latter is lacking. On the other hand, it was reported that a lack of visual attention, or the state of complete inattention, directly affects the dynamics and behaviour of binocular rivalry processes [6, 9]. The authors suggested that new models should consider treating visual attention as an essential parameter linked to binocular rivalry rather than as a modulatory factor. [6, 9].

To conclude, it is important to remark that in 2017, Li et al. devised a binocular rivalry model that took into account the key role of attention in the rivalry process [9]. Their attention model considered three different groups of neurons that were chosen depending on their properties, interrelationships and the activities that they were subjected to within the neuron model [9].

Li et al.'s (2017) model considered that two processes regulated competition in binocular rivalry: visual attention and inhibition between neurons [9]. Attention was modelled as a gain factor that could either be active or inactive depending on whether the individual was attending to a particular stimulus [9]. Moreover, the authors suggested that only a specific group neurons was responsible for the regulation of the attention bias because the other two were respectively focused on receiving and processing the visual inputs and inhibiting competing stimuli, when appropriately [9]. In other words, the model considered visual attention to depend on neural behaviour rather than being a fixed parameter [9]. A more detailed analysis of this model can be found in **Appendix A**, where the interrelationships between neurons are explored more in depth and the equations of the model are presented.

3. Analysis of an existing model of bistable perception: Curtu et al. (2008)

Curtu et al (2008) designed a *firing-rate model* that explored the competition mechanisms of two populations of neurons. They considered that each population caused a negative effect on itself due to neuron fatigue, as well as having the capacity of inhibiting the competitor [5]. The present model is formed by a four-dimensional system of equations with variables u_1, u_2 representing two populations of neurons and a_1, a_2 illustrating the adaptive effect of neurons.

$$\begin{cases} \dot{u_1} = -u_1 + S(I - \beta\, u_2 - g\, a_1), & (7) \\ \dot{u_2} = -u_2 + S(I - \beta\, u_1 - g\, a_2), & (8) \\ \tau\dot{a_1} = -a_1 + u_1, & (9) \\ \tau\dot{a_2} = -a_2 + u_2, & (10) \end{cases}$$

where $S(x) = \dfrac{1}{1 + \exp(-r(x - \theta))}$.

Following the introductory background presented in the Chapter 2, briefly recall that models such as Curtu et al. characterise themselves for the unability of different inputs received by the two eyes to be fused together [4, 5]. Moreover, stimuli will immediately start competing for dominance, causing percepts to continuously and randomly switch states [4, 5].

This chapter of the thesis aims to replicate the quantitative and qualitative analysis of a bistable perception model first proposed by Curtu, Shpiro, Rubin and Rinzel in 2008 and further developed by Curtu in 2010, see [4, 5]. Firstly, it will start by computing the equilibria and bifurcations of the system to then lead into the stability analysis of p^*, the third equilibrium point of the system in which the key bifurcations required to understand the dynamics of the system occur. It was found that it is not feasible to study the other critical points analytically and therefore, we will only discuss these cases numerically.

3.1 Equilibria and bifurcations

In order to start analysing the model and get an overview of the general dynamics of the system, it is mandatory to find the equilibrium points of the system. In other words, we seek to find solutions for $\dot{u_1} = \dot{u_2} = \dot{a_1} = \dot{a_2} = 0$. Thus,

$$\begin{cases} \dot{u_1} = -u_1 + S(I - \beta\, u_2 - g\, a_1) = 0, \\ \dot{u_2} = -u_2 + S(I - \beta\, u_1 - g\, a_2) = 0, \\ \tau\dot{a_1} = -a_1 + u_1 = 0, \\ \tau\dot{a_2} = -a_2 + u_2 = 0. \end{cases} \Rightarrow \begin{cases} u_1 = S(I - \beta\, u_2 - g\, a_1), & (11) \\ u_2 = S(I - \beta\, u_1 - g\, a_2), & (12) \\ a_1 = u_1, & (13) \\ a_2 = u_2. & (14) \end{cases}$$

Considering $F(u)$ to be the inverse function of $S(x)$, that is, $F(u) = \theta + \dfrac{\ln(u/(1-u))}{r}$, the above system of equations can be rewritten as follows.

$$\begin{cases} F(u_1) &= I - \beta\, u_2 - g\, a_1, \\ F(u_2) &= I - \beta\, u_1 - g\, a_2, \\ a_1 &= u_1, \\ a_2 &= u_2. \end{cases} \tag{15}$$

Figure 5 shows a graphical representation of the nullclines of the system (15). The two nullclines intersect three times, concluding that the system will have three possible equilibrium points. Two of the equilibria occur when one population is suppressed by the other which, at the same time, becomes dominant. On the other hand, the third equilibrium point is defined for $u_1 = u_2$, representing a possible change of behaviour on the dynamics of the system; the suppressed population could suddenly become dominant and viceversa. In addition, note that $u_1 = u_2$ implies that $a_1 = u_1$ and $a_2 = u_2$, and thus, this equilibrium point could be expressed as $p^* := (u^*, u^*, u^*, u^*)$.

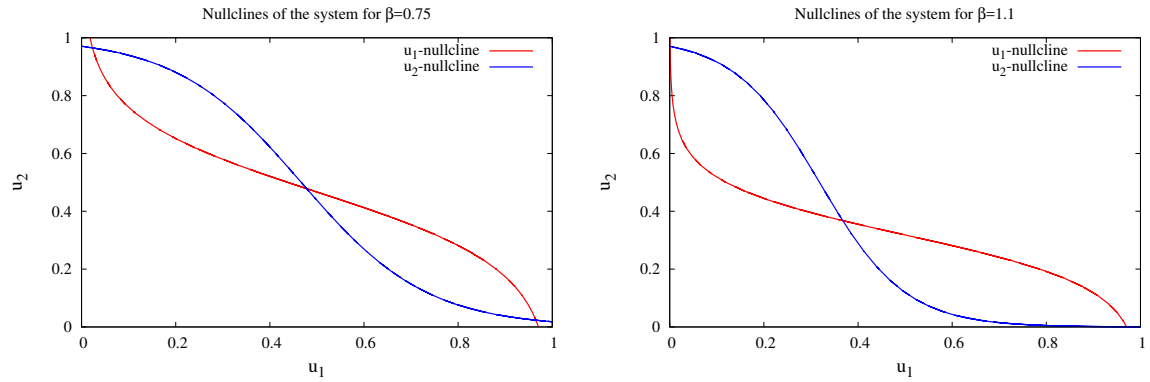

Figure 5: Nullclines for the system taking $g = 0.5$, $I = 0.8$, $\theta = 0.2$ and $r = 10$ for given $\beta = 0.75$ and $\beta = 1.1$, respectively.

By studying the behaviour of p^*, the system can be reduced to only one equation, $F(u) = I - (\beta + g)u$. This equation relates the value/state that the population of neurons will take with respect to the external stimulation of the system, I, the reciprocal inhibition and negative feedback parameters. Therefore, it is easy to see that the above equation could also be written with respect to the input, $I = F(u) + (\beta + g)u$. Moreover, p^* can also give rise to a broader range of dynamics of the system that will be later discussed by exploring other mechanisms such as release and escape.

Nevertheless, at present consider I to be a function that depends on the value of u. Using the basic properties defining the sigmoid function $S(x)$ and its inverse, $F(u)$, we know that $F(u)$ will be monotonically increasing for the interval $(0, 1)$ and that $\lim_{x\to 0} F(u) = -\infty$ whereas $\lim_{x\to 1} F(u) = \infty$ - see Figure 6.

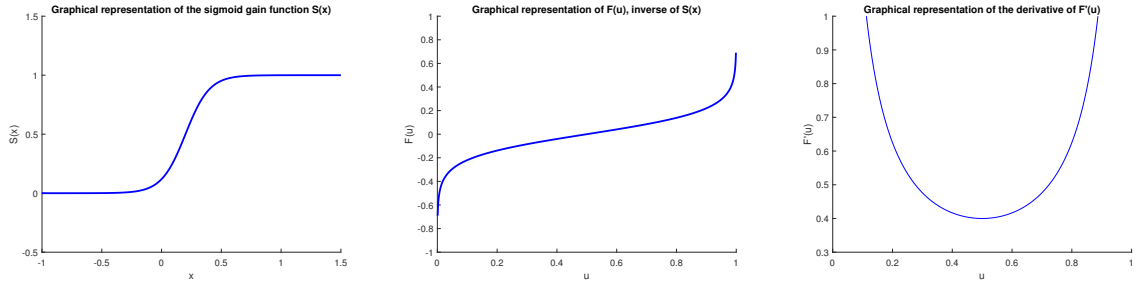

Figure 6: Representation of the sigmoid function S, its inverse F and the derivative of the inverse F'.

Therefore, the above assertion will directly imply that there will be a solution $u^* \in (0, 1)$ for every value of I.

$$I = F(u^*) + (\beta + g)u^*$$

$$dI = [F(u^*) + (\beta + g)]\, du^*$$

$$\frac{du^*}{dI} = \frac{1}{F(u^*) + \beta + g} \tag{16}$$

Overall, the behaviour of the equilibrium point $p^* = (u^*, u^*, u^*, u^*)$ will be characterised by solutions in which the value of u^* directly depends on the external input, I.

3.1.1 Stability analysis of p^*: Preliminary analysis

Next, we want to study the stability of the equilibrium point, $p^* = (u^*, u^*, u^*, u^*)$. For this purpose, recall that we need to compute the eigenvalues of the system and therefore, we will first need to calculate the Jacobian of the system and evaluate it at p^*.

In general,

$$J(u_1, u_2, a_1, a_2) = \begin{pmatrix} \frac{\partial \dot{u_1}}{\partial u_1} & \frac{\partial \dot{u_1}}{\partial u_2} & \frac{\partial \dot{u_1}}{\partial a_1} & \frac{\partial \dot{u_1}}{\partial a_2} \\ \frac{\partial \dot{u_2}}{\partial u_1} & \frac{\partial \dot{u_2}}{\partial u_2} & \frac{\partial \dot{u_2}}{\partial a_1} & \frac{\partial \dot{u_2}}{\partial a_2} \\ \frac{\partial \dot{a_1}}{\partial u_1} & \frac{\partial \dot{a_1}}{\partial u_2} & \frac{\partial \dot{a_1}}{\partial a_1} & \frac{\partial \dot{a_1}}{\partial a_2} \\ \frac{\partial \dot{a_2}}{\partial u_1} & \frac{\partial \dot{a_2}}{\partial u_2} & \frac{\partial \dot{a_2}}{\partial a_1} & \frac{\partial \dot{a_2}}{\partial a_2} \end{pmatrix} =$$

$$= \begin{pmatrix} -1 & -\beta S'(I - \beta\, u_2 - g\, a_1) & -gS'(I - \beta\, u_2 - g\, a_1) & 0 \\ -\beta S'(I - \beta\, u_1 - g\, a_2) & -1 & 0 & -gS'(I - \beta\, u_1 - g\, a_2) \\ 1/\tau & 0 & -1/\tau & 0 \\ 0 & 1/\tau & 0 & -1/\tau \end{pmatrix}.$$

Evaluating the Jacobian at the equilibrium point p^*, we obtain

$$J(u^*,u^*,u^*,u^*) = \begin{pmatrix} -1 & -\beta\, S'(x) & -g\, S'(x) & 0 \\ -\beta\, S'(x) & -1 & 0 & -g\, S'(x) \\ 1/\tau & 0 & -1/\tau & 0 \\ 0 & 1/\tau & 0 & -1/\tau \end{pmatrix} = \begin{pmatrix} -1 & \frac{-\beta}{F'(u^*)} & \frac{-g}{F'(u^*)} & 0 \\ \frac{-\beta}{F'(u^*)} & -1 & 0 & \frac{-g}{F'(u^*)} \\ 1/\tau & 0 & -1/\tau & 0 \\ 0 & 1/\tau & 0 & -1/\tau \end{pmatrix}.$$

The next step of the analysis requires finding the eigenvalues associated to this equilibrium point in order to determine its stability. Firstly, the characteristic polynomial is given by

$$X_A(t) = \det \begin{bmatrix} -1-\lambda & \frac{-\beta}{F'(u^*)} & \frac{-g}{F'(u^*)} & 0 \\ \frac{-\beta}{F'(u^*)} & -1-\lambda & 0 & \frac{-g}{F'(u^*)} \\ 1/\tau & 0 & -1/\tau-\lambda & 0 \\ 0 & 1/\tau & 0 & -1/\tau-\lambda \end{bmatrix} = 0, \tag{17}$$

and thus,

$$X_A(t) = (-1-\lambda)\begin{vmatrix} -1-\lambda & 0 & \frac{-g}{F'(u^*)} \\ 0 & -\frac{1}{\tau}-\lambda & 0 \\ 1/\tau & 0 & -\frac{1}{\tau}-\lambda \end{vmatrix} + \frac{\beta}{F'(u^*)}\begin{vmatrix} \frac{-\beta}{F'(u^*)} & \frac{-g}{F'(u^*)} & 0 \\ 0 & -\frac{1}{\tau}-\lambda & 0 \\ 1/\tau & 0 & \frac{1}{\tau}-\lambda \end{vmatrix} + \frac{1}{\tau}\begin{vmatrix} \frac{-\beta}{F'(u^*)} & \frac{-g}{F'(u^*)} & 0 \\ -1-\lambda & 0 & \frac{-g}{F'(u^*)} \\ \frac{1}{\tau} & 0 & -\frac{1}{\tau}-\lambda \end{vmatrix}$$

$$= (-1-\lambda)\left[(-1-\lambda)\left(-\frac{1}{\tau}-\lambda\right)^2 + \frac{g}{\tau F'(u^*)}\left(-\frac{1}{\tau}-\lambda\right)\right] + \frac{\beta}{F'(u^*)}\left[-\frac{\beta}{F'(u^*)}\left(-\frac{1}{\tau}-\lambda\right)^2\right]$$

$$+ \frac{1}{\tau}\left[\frac{1}{\tau}\left(\frac{g}{F'(u^*)}\right)^2 + \frac{g}{F'(u^*)}(-1-\lambda)\left(-\frac{1}{\tau}-\lambda\right)\right]$$

$$= (-1-\lambda)^2\left(-\frac{1}{\tau}\right)^2 + \frac{-g(1+\lambda)}{\tau F'(u^*)}\left(-\frac{1}{\tau}\right) - \left[\frac{\beta}{F'(u^*)}\left(\lambda+\frac{1}{\tau}\right)^2\right] + \left(\frac{g}{\tau F'(u^*)}\right)^2 + \frac{-g(1+\lambda)}{\tau F'(u^*)}\left(-\frac{1}{\tau}-\lambda\right)$$

$$= \left[(\lambda+1)\left(\lambda+\frac{1}{\tau}\right)\right]^2 + 2\frac{g}{\tau F'(u^*)}(\lambda+1)\left(\lambda+\frac{1}{\tau}\right) + \left[\frac{g}{\tau F'(u^*)}\right]^2 - \left[\frac{\beta}{F'(u^*)}\left(\lambda+\frac{1}{\tau}\right)\right]^2$$

$$= \left[(\lambda+1)\left(\lambda+\frac{1}{\tau}\right) + \frac{g}{\tau F'(u^*)}\right]^2 - \left[\frac{\beta}{F'(u^*)}\left(\lambda+\frac{1}{\tau}\right)\right]^2 = 0 \tag{18}$$

The algebraic identity $a^2 - b^2 = (a+b)(a-b)$ allows to rewrite (18) as the product of two quadratic equations. This fact will simplify the computations to obtain the associated eigenvalues.

$$\left[(\lambda+1)\left(\lambda+\frac{1}{\tau}\right)+\frac{g}{\tau F'(u^*)}+\frac{\beta}{F'(u^*)}\left(\lambda+\frac{1}{\tau}\right)\right]\left[(\lambda+1)\left(\lambda+\frac{1}{\tau}\right)+\frac{g}{\tau F'(u^*)}-\frac{\beta}{F'(u^*)}\left(\lambda+\frac{1}{\tau}\right)\right]=0$$

Expanding the first term as a quadratic equation gives the following result.

$$\left[(\lambda+1)\left(\lambda+\frac{1}{\tau}\right)+\frac{g}{\tau F'(u^*)}+\frac{\beta}{F'(u^*)}\left(\lambda+\frac{1}{\tau}\right)\right]=0$$

$$\Rightarrow\ \lambda^2+\left(\frac{1}{\tau}+1+\frac{\beta}{F'(u^*)}\right)\lambda+\frac{1}{\tau}\left(1+\frac{1}{F'(u^*)}(g+\beta)\right)=0 \tag{19}$$

Similarly, for the second term,

$$\left[(\lambda+1)\left(\lambda+\frac{1}{\tau}\right)+\frac{g}{\tau F'(u^*)}-\frac{\beta}{F'(u^*)}\left(\lambda+\frac{1}{\tau}\right)\right]=0$$

$$\Rightarrow\ \lambda^2+\left(\frac{1}{\tau}+1-\frac{\beta}{F'(u^*)}\right)\lambda+\frac{1}{\tau}\left(1+\frac{1}{F'(u^*)}(g-\beta)\right)=0 \tag{20}$$

Last, it is only left to find the eigenvalues associated to the characteristic polynomial. Given that in both cases (19) and (20) are quadratic equations of the form $\lambda^2 - t\lambda + d = 0$, the associated eigenvalues will be computed as follows

$$\lambda=\frac{-t\pm\sqrt{t^2-4d}}{2} \tag{21}$$

Firstly, (19) is solved by substituting $t=-\left(\frac{1}{\tau}+1+\frac{\beta}{F'(u^*)}\right)$ and $d=\frac{1}{\tau}\left(1+\frac{1}{F'(u^*)}(g+\beta)\right)$ into (21). It is easy to see that $t<0$ and $d>0$ independently of the value of the parameters, which concludes that λ_1, λ_2 will be eigenvalues with positive real part independently of the external input applied to the system. On the other hand, (20) is solved by substituting $t=-\left(\frac{1}{\tau}+1-\frac{\beta}{F'(u^*)}\right)$ and $d=\frac{1}{\tau}\left(1+\frac{1}{F'(u^*)}(g-\beta)\right)$ into (21). In this case, however, the value and sign of t and d is not trivial as for some parameter values λ_3 and λ_4 may give rise to some bifurcation dynamics.

Thus, the equilibrium point p^* will be stable, and therefore an attractor, if the inequalities $F'(u^*) > \frac{\beta}{\frac{1}{\tau}+1}$ and $F'(u^*) > \beta - g$ are satisfied. On the other hand, we will have unstable equilibria, sometimes in the form of a bifurcation, when any of the two the inequalities are not satisfied. Moreover, depending on the relationship between the criteria defining the two bifurcations, i.e. which one occurs first, the relationship between the parameters of the model may change.

Assume that the two eigenvalues of the system corresponding to (20) are of the form $\lambda_j = a + (-1)^j\, b\, i$ for $j = 3, 4$, where a and b depend on the parameters of the system. We recall that a **Hopf bifurcation** with respect to a parameter ξ would occur if $a = a(\xi_0) = 0$ and $b(\xi_0) \neq 0$ for some $\xi \in (\xi_0 - \xi, \xi + \xi_0)$ as well as satisfying $\frac{\partial}{\partial \xi} t(\xi_0) \neq 0$ - also known as the *transversality hypothesis*.

In this particular case, as both eigenvalues are calculated using (21), constraints (23) and (24) will need to be satisfied in order for a Hopf bifurcation to occur (22).

$$t^2 - 4d < 0 \;\text{ for any }\; \xi \in (\xi_0 - \xi, \xi + \xi_0) \tag{22}$$

$$t(\xi_0) = 0 \;\Rightarrow\; d(\xi_0) = \frac{t^2}{4} > 0 \tag{23}$$

$$\frac{\partial}{\partial \xi} t(\xi_0) \neq 0 \tag{24}$$

Firstly, as it will be shown in subsection 3.1.2, the simple form of $F'(u)$ ensures that the *transversality hypothesis*, (24), is satisfied. Therefore, it is only left to show that conditions (22) and (23) hold to conclude that a Hopf bifurcation occurs in the system.

$$-\left(\frac{1}{\tau} + 1 - \frac{\beta}{F'(u^*)}\right) = 0 \;\Rightarrow\; F'(u^*) = \frac{\beta}{\frac{1}{\tau} + 1} \tag{25}$$

$$\frac{1}{\tau}\left(1 + \frac{1}{F'(u^*)}(g - \beta)\right) > 0 \;\Rightarrow\; F'(u^*) > \beta - g \tag{26}$$

Thus, when (25) and (26) are satisfied the dynamics of the system will be influenced by a Hopf bifurcation.

On the other hand, the bifurcation diagrams that will be later discussed in section 3.3 also show that the system contains a Pitchfork bifurcation for some values of I. Following Curtu et al.'s analysis of the model, it was hypothesised that the bifurcation would take place when the value of one of the eigenvalues was null. In other words, it is necessary that $d = 0$ in (21) for a Pitchfork bifurcation to occur.
Thus, it would need to satisfy

$$\frac{1}{\tau}\left(1 + \frac{1}{F'(u^*)}(g - \beta)\right) = 0 \;\Rightarrow\; F'(u^*) = \beta - g \tag{27}$$

Moreover, a Hopf bifurcation will occur first when $\frac{\beta}{\frac{1}{\tau}+1} > \beta - g$.

$$\beta > (\beta - g)\left(\frac{\tau + 1}{\tau}\right) \;\Rightarrow\; \beta\left(1 - \frac{\tau + 1}{\tau}\right) > -g\left(\frac{\tau + 1}{\tau}\right) \;\Rightarrow\; \frac{\beta}{g} < 1 + \tau \tag{28}$$

In contrast, if $\frac{\beta}{\frac{1}{\tau}+1} < \beta - g$ holds, the system will first encounter a Pitchfork bifurcation.

$$\beta < (\beta - g)\left(\frac{\tau+1}{\tau}\right) \quad \Rightarrow \quad \beta\left(1 - \frac{\tau+1}{\tau}\right) < -g\left(\frac{\tau+1}{\tau}\right) \quad \Rightarrow \quad \frac{\beta}{g} > 1+\tau \tag{29}$$

If (28) is satisfied, the value of the eigenvalues λ_3, λ_4 would radically change from being negative and real to acquiring complex and imaginary values. On the other hand, if (29) held instead, the negative and real eigenvalues belonging to the system would change in a way such that one of them was null and the other was still negative and real.

To sum up, it is important to recall that the model initially considered the parameter τ as representing large values, $\tau >> 1$. This implies that, in order to satisfy this constraint, we require $\frac{\beta}{g} << \tau$ and therefore, it is more convenient to use (28).

$$\frac{\beta}{g} > 1+\tau \quad \Rightarrow \quad \beta > g\,(1+\tau) \tag{30}$$

Psychophysically speaking, the relationship satisfied by $\beta > g\,(1+\tau)$ could imply that the current model has a higher adaptation strength than inhibition, and therefore, that the negative feedback component of the neurons is more prominent.

3.1.2 Stability analysis of p^*: Dynamics illustrating a Hopf bifurcation

This subsection will analyse the behaviour of the system by considering the parameters τ, g fixed and varying the values of β. Moreover it aims to graphically prove the *transversality hypothesis* in order to justify the existence of a Hopf bifurcation. Firstly, it is important to remark that due to the form of the sigmoid function $S(x)$, the inverse of its inverse function $F(u)$ will be defined as $F'(u) = \frac{1}{S'(\theta)}$. By definition, for any function we have a minimum when its derivative it is equal to 0. Therefore, in this case, $F'(u)$ will have a minimum at $\frac{1}{S'(\theta)}$ due to $F''(u) = 0$.

Furthermore, recall that (30) proposed an optimal relationship between the time constant, adaptation and inhibition variables of the problem such that it satisfied $\tau >> 1$. This fact also assumed that the change of stability in the system would firstly arise through a Hopf bifurcation that occurred when $F'(u^*) = \frac{\beta}{1+\frac{1}{\tau}}$. Notice that the form of the condition that needs to be satisfied corresponds to a straight line and therefore, the changes of stability will occur in the intersections between (25) and the general form of the $F'(u)$ curve. This concludes that depending on the value that β takes, the system may have different dynamics.

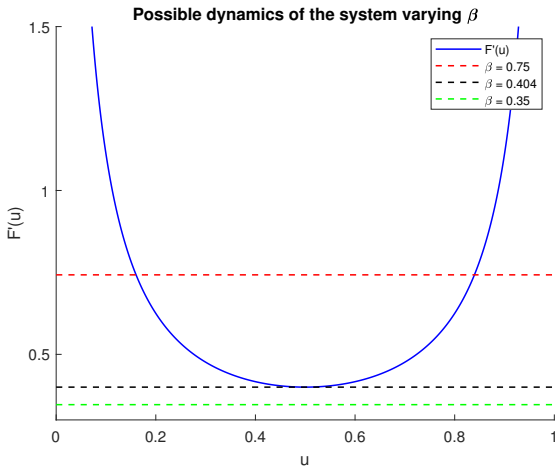

Figure 7: Representation of the possible dynamics of the system varying the value of β

Figure 7 shows that there exists three possible dynamics that depend on the number of times that the line satisfying (25) crosses the general $F'(u)$ curve.

- ⋆ When $\frac{\beta}{1+\frac{1}{\tau}} = \frac{1}{S'(\theta)}$, the graphs only intersect once, as the intersection point is located at the minimum extrema of $F'(u)$. This inflection point on the dynamics occurs when $\beta = \frac{1+\frac{1}{\tau}}{S'(\theta)}$.
  As the general expression of $F'(u)$ has been plotted for $\beta = 1.1$, the limiting value of β corresponds to $\beta = 0.404$. This case would correspond to a co-dimension two bifurcation.
- ⋆ When $\frac{\beta}{1+\frac{1}{\tau}} < \frac{1}{S'(\theta)}$ there exists no intersections between the curve $F'(u)$ and the line $F'(u) = \frac{1}{S'(\theta)}$ and therefore, no Hopf bifurcations will arise for these particular values of β. This situation is exemplified by the green dashed line in which $\beta = 0.35$.
- ⋆ When $\frac{\beta}{1+\frac{1}{\tau}} > \frac{1}{S'(\theta)}$, Figure 7 shows that the corresponding line for $\beta = 0.75$ intersects twice with the $F'(u)$ curve. Thus, considering u_{HBA} and u_{HBB} the intersection points with the curves, it can be easily concluded that $u_{HBA}, u_{HBB} \in (0, 1)$ and that $u_{HBA} < u_{HBB}$ due to the shape of the general curve $F'(u)$. In addition, u_{HBA}, u_{HBB} will also satisfy

$$F'(u_{HBA}) = F'(u_{HBB}) = \frac{\beta}{1+\frac{1}{\tau}}$$

  In other words, $F'(u_{HBA})$ and $F'(u_{HBB})$ will represent the associated values of two Hopf bifurcation points which will influence an abrupt change on the stability of the system. Moreover, the *transversality condition* for a Hopf bifurcation to occur is also geometrically satisfied because the $F'(u)$ curve is being intersected by a straight line. The system will tend to oscillate between these two Hopf bifurcation points, directly implying that the system requires $\beta > \frac{1+\frac{1}{\tau}}{S'(\theta)}$ for oscillations to occur.

3.2 An introduction to release, escape and Winner-Take-All mechanisms

Previous sections have defined and discussed the general behaviour of a competitive neuron model. Recall that in models such as the one that is being considered in this report, populations are either dominant or inhibited [5]. For that reason, both populations will tend to oscillate until a complete dominant state is achieved. This section will introduce specific dynamical behaviours, such as release and escape mechanisms, that have been found to abruptly cause a change in the behaviour of neuron populations. Explanations and discussions will be introduced through a toy example of the original model that uses a Heaviside function in order to carefully illustrate the dynamical regimes that lead to mechanisms of release, escape and Winner-Take-All.

Definition 3.1. In neuroscience, a **release mechanism** refers to an sudden depression of the active population. In other words, the activity of the dominating percept abruptly stops, no longer suppressing the competitor [5].

Definition 3.2. An **escape mechanism** occurs when the suppressed population suddenly becomes active and dominant, forcing the other population to an inhibition state [5]. In other words, this mechanism refers to an abrupt potentiation of the suppressed population. For that reason, escape mechanisms can be seen for high values of the external input parameter, I.

Definition 3.3. Winner-Take-All dynamics occur when the system no longer oscillates, forcing neuron populations to remain in their dominant or suppressed state indefinitely, or until an abrupt change in the parameters takes place [5].

3.2.1 A toy example: Heaviside function

For an easier and deeper explanation of the mechanisms underlying a competitive neuron model, a Heaviside function of the form $S(x) = Heav(x-\theta) = \begin{cases} 0 & \text{if } x < \theta \\ 1 & \text{if } x > \theta \end{cases}$ has been considered.
Therefore, the present competition model will now be structured as

$$\begin{cases} \dot{u_1} = -u_1 + H(I - \beta\, u_2 - g\, a_1) = 0 & (31) \\ \dot{u_2} = -u_2 + H(I - \beta\, u_1 - g\, a_2) = 0 & (32) \\ \tau \dot{a_1} = -a_1 + u_1 = 0 & (33) \\ \tau \dot{a_2} = -a_2 + u_2 = 0 & (34) \end{cases}$$

where $H(I - \beta u - ga) = \begin{cases} 0 & \text{if } I - \beta u - ga < \theta \\ 1 & \text{if } I - \beta u - ga > \theta \end{cases}$

Computing the nullclines of the system, gives the opportunity to the reader to easily see that the model may have four different equilibrium points, depending on whether the two fast variables either take value 0 or 1.

- u_1−**nullcline:** $\frac{du_1}{dt} = 0$: $u_1 = H(I - \beta\, u_2 - g\, a_1)$
- u_2−**nullcline:** $\frac{du_2}{dt} = 0$: $u_2 = H(I - \beta\, u_1 - g\, a_2)$

In other words, the system may have the following equilibria : $P_1^* = (1, 1, 1, 1)$, $P_2^* = (1, 0, 1, 0)$, $P_3^* = (0, 1, 0, 1)$ and $P_4^* = (0, 0, 0, 0)$. Note that the only two equilibrium points that could give rise to oscillations are P_2^* and P_3^* because in both cases one of the populations is being inhibited by the other to ensure dominance. Moreover, one could suggest that both P_2^* and P_3^* satisfy that

$$u_1 + u_2 = 1 \tag{35}$$

and therefore that oscillatory solutions will arise when the previous condition is satisfied [5]. Furthermore, by substituting (35) in the resulting addition of equations (33) and (34), one can model the behaviour of the slow variables and their dynamics with respect to their corresponding fast variables.

$$\tau\left(\frac{da_1}{dt} + \frac{da_2}{dt}\right) = -a_1 - a_2 + u_1 + u_2$$

$$\tau\left(\frac{da_1}{dt} + \frac{da_2}{dt}\right) = -(a_1 + a_2) + 1 \tag{36}$$

Thus, the general behaviour of the slow variables can be computed by setting (36) equal to zero.

$$a_1 + a_2 = 1 \tag{37}$$

Equation (37) illustrates the fact that the relationship between the slow dynamics can be represented within a square of unit length as variables a_1 and a_2 can take any value between zero and one. Moreover, it is interesting to remark that the oscillatory dynamics associated to a_1 and a_2 would only occur on the straight line satisfying (37), as shown in Figure 8.

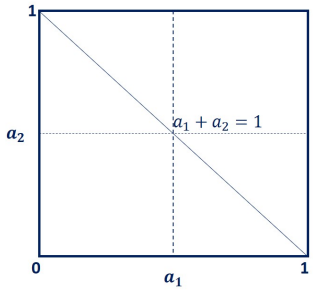

Figure 8: Graphical representation for the space of dynamics of the slow variables

On the other hand, it is easy to see that due to the properties associated to the Heaviside function, the situation satisfying $I - \beta\, u_j - g\, a_i = \theta$ could represent an inflection on the system's dynamics. Curtu et al. (2008) suggest that this turning point is present on the system in the form of a threshold associated to each

nullcline [5]. In particular, the u_1-nullcline would have a threshold value associated to $I - \beta\, u_2 - g\, a_1 = \theta$.

$$I - \beta\, u_2 - g\, a_1 = \theta \quad \Rightarrow \quad I - (\theta + g\, a_1) = \beta\, u_2 \quad \Rightarrow \quad u_2 = \frac{I - (\theta + g\, a_1)}{\beta} \tag{38}$$

Similarly, the inflection value associated to the u_2-nullcline would be calculated by setting $I - \beta\, u_1 - g\, a_2 = \theta$.

$$I - \beta\, u_1 - g\, a_2 = \theta \quad \Rightarrow \quad I - (\theta + g\, a_2) = \beta\, u_1 \quad \Rightarrow \quad u_1 = \frac{I - (\theta + g\, a_2)}{\beta} \tag{39}$$

The expressions obtained in (38) and (39) imply that the system will have a general threshold point of the form

$$P_{thres} = \left(\frac{I - (\theta + g\, a_2)}{\beta}, \frac{I - (\theta + g\, a_1)}{\beta} \right) \tag{40}$$

The expression of equation (40) directly depends on the values given for the slow variables and the parameters β, θ, I, g. Thus, any change on the slow variables, even if the model is always evaluated using constant parameters, will directly influence the value and corresponding position of (40) along the vertical or horizontal axes [5].

Moreover, it is interesting to highlight that there exists two different expressions for a_1 and a_2 associated to the system's threshold point that, if reached, could cause the behaviour of the solution to immediately switch. These expressions are called **jumping values** because they induce the fast variables u_1, u_2 to suddenly change from an active to a suppressed state. For example, a_1^* would represent the jumping value associated to the u_1-nullcline's threshold and, similarly, a_2^* would belong to u_2.

1. $u_1 = 1$ **and** $u_2 = 0$ **switch to** $u_1 = 0$ **and** $u_2 = 1$

   The present case models the situation in which the fast variable u_1 is abruptly suppressed while u_2 is being potentiated, i.e. $u_1 = 0$ and $u_2 = 1$. It occurs when a_1 and a_2 reach the threshold point of the system defined in (40). Thus, the expression for the jumping points a_1^*, a_2^*, can be found by considering that the inflection point will be satisfied for the turning values $u_1 = 1$ and $u_2 = 0$ just before the switch.

$$u_2 = \frac{I - (\theta + g\, a_1)}{\beta} = 0 \quad \Rightarrow \quad I - \theta - g\, a_1 = 0 \quad \Rightarrow \quad a_1^* = \frac{I - \theta}{g} \tag{41}$$

$$u_1 = \frac{I - (\theta + g\, a_2)}{\beta} = 1 \quad \Rightarrow \quad I - \theta - g\, a_2 = \beta \quad \Rightarrow \quad a_2^* = \frac{I - (\theta + \beta)}{g} \tag{42}$$

2. $u_1 = 0$ **and** $u_2 = 1$ **switch to** $u_1 = 1$ **and** $u_2 = 0$

   Similarly, the jumping points associated to the sudden activation and suppression of the corresponding fast variables u_1 and u_2 will be computed by evaluating the threshold values of the u_1-nullcline and u_2-nullcline at 1 and 0, respectively.

$$u_2 = \frac{I - (\theta + g\, a_1)}{\beta} = 1 \quad \Rightarrow \quad I - \theta - g\, a_1 = \beta \quad \Rightarrow \quad a_1^* = \frac{I - (\theta + \beta)}{g} \tag{43}$$

$$u_1 = \frac{I - (\theta + g\, a_2)}{\beta} = 0 \quad \Rightarrow \quad I - \theta - g\, a_2 = 0 \quad \Rightarrow \quad a_2^* = \frac{I - \theta}{g} \tag{44}$$

From equations (41), (42), (43) and (44), it is easy to see that the system will have two jumping points associated to each slow variable and that their expressions will be related such that $\frac{I-(\theta-\beta)}{g} < \frac{I-\theta}{g}$. Moreover, the jumping values will give the opportunity to determine whether the system is under a release or an escape mechanism depending on which of the two expressions associated to a_1 and a_2 is reached first [5].

On the one hand, recall that a release mechanism occurs between two competing populations of neurons when the active population suddenly switches to a suppressed state by allowing the inhibited one to become active. Therefore, the jumping value constraint causing this phenomenon would be $a_R = \frac{I-\theta}{g}$. On the other hand, the escape mechanism between two competing populations of neurons occurs when the population that is being inhibited abruptly switches state and becomes active, reciprocally suppressing the opponent percept. Thus, the expression satisfying $a_E = \frac{I-(\theta+\beta)}{g}$ could be considered as the regulatory constraint determining this mechanism.

Finally, by considering β, θ and g as fixed parameters and the input strength I as a variable, the jumping expressions could be represented as straight lines that respectively model the switches between the active and suppressed states of the two fast variables. As a result, the switches in dynamics for this system would occur on the area defined by the four straight lines representing the jumping values for a_1 and a_2 - see Figure 9.

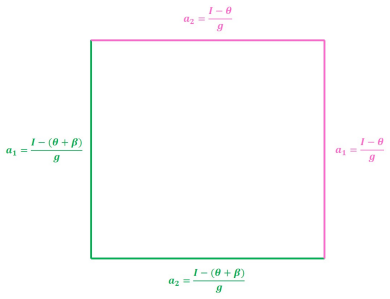

Figure 9: Graphical representation of the area of dynamics delimited by the jumping points

Dynamics of the model for different values of β

This last section will explore the different changes on the dynamics with respect to the positions that the square of jumping points can adopt within the unit square. In other words, the analysis will discuss the different dynamics that occur when the two squares intersect, recalling that oscillatory solutions will only occur if (37) is crossed [5].

It is important to note that the dynamical regimes belonging to this system will depend on the relationship between the relative sizes of the two squares; 1 and $\frac{\beta}{g}$, respectively. In other words, if $\frac{\beta}{g} < 1$, the range of values for which the jumping values' square is defined will be smaller than 1, whereas $\frac{\beta}{g} > 1$ would imply that the unit square is smaller in area. Note that the relative size of the square modelling the jumping dynamics is calculated by subtracting (42) from (41).

In order to provide the reader with a general overview of the dynamics of the model, the section will only consider the case $\frac{\beta}{g} > 1$, as it shows a broader range of dynamical behaviours. In addition, Curtu et al [5] defined that when $\frac{\beta}{g} > 1$ the two squares could intersect in seven different manners and therefore, there could be seven possible dynamical regimes. However, at the end of the section we will conclude that although there are seven possible regimes, only five of them represent different dynamics [5].

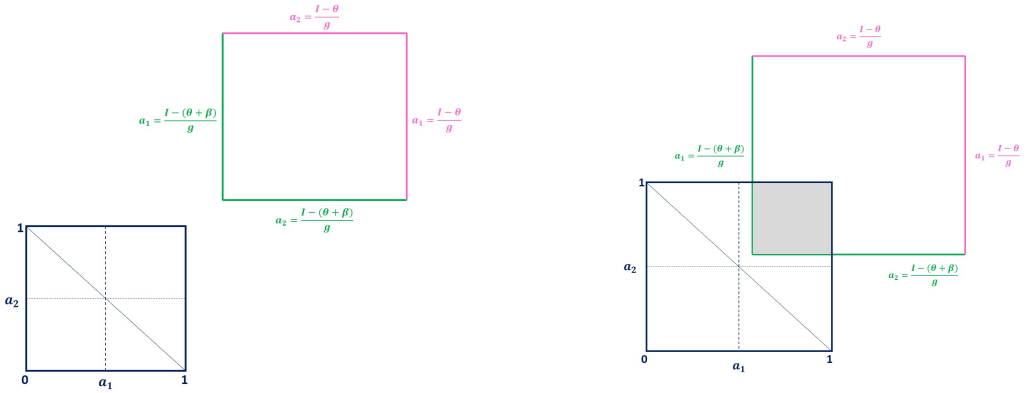

Figure 10: Graphical representation for **Regime 1** (left) and **Regime 2** (right)

⋆ **Regime 1:** $1 \leq \frac{I-(\theta-\beta)}{g} < \frac{I-\theta}{g}$

Figure 10 (left) shows that this first case corresponds to the situation in which the *jumping dynamics square* lies outside the square of slow variables and it is defined for values greater than 1. Moreover, in this case the two squares do not intersect and thus, the dynamics of the system for this interval will not represent any oscillatory dynamics or big switches in dominance.

Using the limiting values that define this regime it can be argued that, if $1 \leq \frac{I-(\theta-\beta)}{g}$, then $I - \beta - g \geq \theta$. In addition, recall that the values of u_1 and u_2 for this system will be given by the expression of its nullclines; i.e. $u_1 = H(I - \beta\, u_2 - g\, a_1)$ and $u_2 = H(I - \beta\, u_1 - g\, a_2)$ which take

value one or zero depending on whether $I - \beta\, u_j - g\, a_i$ is greater or smaller than a given θ.

Considering that $(u_1, u_2, a_1, a_2) \in (0, 1)$ and that i and j are subindices representing opposite population on neurons, it is easy to see that the following inequalities will always hold.

$$I - \beta\, u_j - g\, a_i \geq I - \beta - g \geq \theta \tag{45}$$

Thus, it can be concluded that, due to the properties of the Heaviside function and for any associated value of the slow variables, the associated fast variable will take value 1. Needless to say, (u_1, u_2) will represent the only attractor point of the system defined for any value of I that satisfies $1 \leq \frac{I-(\theta-\beta)}{g} < \frac{I-\theta}{g}$.

⋆ **Regime 2:** $\frac{1}{2} \leq \frac{I-(\theta-\beta)}{g} < 1 < \frac{I-\theta}{g}$

From this regime onwards, we will assume that the initial condition corresponds to a bistable case, so that we can later discuss where the fast variables will tend to. Recall that, by definition, the slow variables model the adaptation factor and as such, they represent a negative influence to the fast variable [5]. Therefore, if we want to suppress/activate u_1 in order to activate/suppress u_2, we require a_1 to increase/decrease and a_2 to decrease/increase on value [5].

Figure 10 (right) graphically represents the position of the two squares with respect to each other for this particular regime. First, we assume that the system is initialised with $(u_1, u_2) = (1, 0)$. Then, due to the properties of the system, the slow variables a_1 and a_2 will start to respectively increase and decrease as it has been just discussed [5].

In addition, as the dynamics that are being considered in this regime can only occur inside the grey square in Figure 10 (right), the only possible jumping point that could be reached to switch the dynamics established is $a_2^* = \frac{I-(\theta+\beta)}{g}$. If this crossing occurs, u_2 will be activated just after the jump. However, $u_2 = 1$ does not ensure u_1 becoming inactive and taking value 0.

By definition, the associated value of u_1 just after the jump can be calculated by considering $u_1 = H(I - \beta\, u_2 - g\, a_1)$, $u_2 = 1$ and $a_1 = 1 - a_2^*$.

$$I - \beta\, u_2 - g\, a_1 = I - \beta\, u_2 - g(1 - a_2^*) = I - \beta - g\left(1 - \frac{I - (\theta + \beta)}{g}\right) = 2I - 2\beta - \theta - g \tag{46}$$

Moreover, recall that the dynamics for this case are only defined for the following limiting values; $\frac{1}{2} \leq \frac{I-(\theta-\beta)}{g} < 1 < \frac{I-\theta}{g}$. Rearranging the inequality for $\frac{1}{2} \leq \frac{I-(\theta-\beta)}{g}$ it is easy to see that the expression is equivalent to saying that $2I - 2\beta - g \geq 2\theta$. Thus, Equation (46) also satisfies that

$$I - \beta\, u_2 - g\, a_1 = 2I - 2\beta - \theta - g \geq \theta$$

which directly implies that $u_1 = H(I - \beta\, u_2 - g\, a_1) = 1$. Similarly to **Regime 1**, it can therefore be concluded that if the jumping lines are defined such that $\frac{1}{2} \leq \frac{I-(\theta-\beta)}{g} < 1 < \frac{I-\theta}{g}$, the system will only have one attractor point in which both populations will become active.

Remark 3.4. Note that if the initial condition $(u_1, u_2) = (0, 1)$ was considered instead, although the same argument and results would apply, the only possible jumping point that could be crossed would be $a_1^* = \frac{I-(\theta+\beta)}{g}$.

⋆ **Regime 3:** $0 < \frac{I-(\theta-\beta)}{g} < \frac{1}{2} < 1 < \frac{I-\theta}{g}$

Regime 3 considers the situation when the square of jumping points crosses the unit square through the main diagonal that defines the oscillatory dynamics. Because of this particular crossing, one would expect for oscillations to arise when $0 < \frac{I-(\theta-\beta)}{g} < \frac{1}{2} < 1 < \frac{I-\theta}{g}$, i.e. $I - \beta > \theta$, $I - g < \theta$ and $2I - 2\beta - g < \theta$.

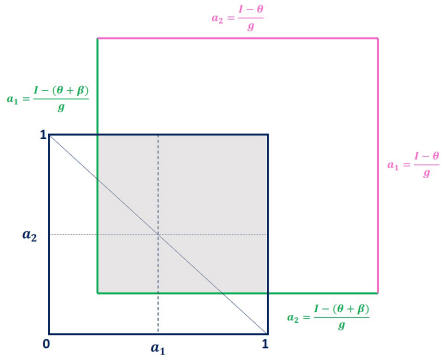

Figure 11: Graphical representation for **Regime 3**

If the system is initially defined such that $u_1 = 1, u_2 = 0$, the associated slow variables would tend to increase and decrease their values, respectively. Looking at the graphical representation of the regime shown in Figure 11, it is easy to see that if a_1 and a_2 follow the behaviour described above, the only jumping line that could be crossed and cause an abrupt change on the dynamics would be $a_2^* = \frac{I-(\theta+\beta)}{g}$.

If the above happened, u_2 would be instantly activated and take value 1. However, as discussed in previous regimes, the value that u_1 would take could differ depending on the limiting values that defined the jumping lines. Therefore, u_1 would need to be computed by using the fact that $u_1 = H(I - \beta\, u_2 - g\, a_1)$ and $a_1 = 1 - a_2^*$ just after the jump.

$$I - \beta\, u_2 - g\, a_1 = I - \beta - g\left(1 - \frac{I - (\theta + \beta)}{g}\right) = 2I - 2\beta - g - \theta < \theta \tag{47}$$

Equation (47) implies that just after the jump $(u_1, u_2) = (0, 1)$, causing an abrupt switch on the dynamics belonging to the fast variables. Moreover, as $(u_1, u_2) = (0, 1)$ does not correspond to an attractor point, the system will continue to oscillate. However, the behaviour of the slow variables will abruptly switch after the jump, inducing the values of a_1 to decrease and a_2 to increase. For that reason, it can be concluded that the system will reach $(u_1, u_2) = (1, 0)$ again but only by crossing the jumping line for $a_1^* = \frac{I-(\theta+\beta)}{g}$.

Thus, it could be concluded that **Regime 3** represents an oscillatory dynamics case for this problem. Moreover, it is important to remark that both fast variables drastically switched states during the oscillations by crossing two jumping lines which were both defined by $\frac{I-(\theta+\beta)}{g}$. For that reason, **Regime 3** could be thought to exemplify an **escape mechanism**.

Finally, for escape mechanisms, one can calculate the period for which they will occur. Start by considering the equations defining the slow variables' dynamics.

$$\tau \frac{da_2}{dt} = -a_2 + u_2 \quad \Rightarrow \quad \tau \frac{da_2}{dt} = -a_2 \tag{48}$$

Integrating the above equation we obtain

$$\int \frac{1}{a_2} da_2 = \int -\frac{1}{\tau} dt$$

$$\ln(a_2) = -\frac{1}{\tau} t + C$$

$$a_2(t) = a_i e^{-\frac{t}{\tau}}, \quad t \in \left(0, \frac{T}{2}\right) \tag{49}$$

Due to the fact that any solution for this equation needs to satisfy (48), we have set the initial condition of the system to be a_i in (49). Therefore, the period of oscillation can now be computed by substituting $t = \frac{T}{2}$ into (49).

$$\frac{a_2}{a_i} = e^{-\frac{T}{2\tau}}$$

$$\ln\left(\frac{a_i}{a_2}\right) = \frac{T}{2\tau}$$

$$T = 2\tau \ln\left(\frac{a_i}{a_2}\right) \tag{50}$$

Considering that the value of the slow variable a_2 just after the jump satisfies $1 - a_1^*$ and that the escape mechanism associated to (48) occurs when a_2^* reaches the line $a_E = \frac{I-(\theta+\beta)}{g}$, equation (50) can be rewritten as follows to define the period of escape, T_{escape}.

$$T = 2\tau \ln\left(\frac{1-a_1^*}{a_2^*}\right) = 2\tau \ln\left[\left(1 - \frac{I-(\theta+\beta)}{g}\right) \cdot \frac{g}{I-(\theta+\beta)}\right] =$$

$$= 2\tau \ln\left[\frac{g}{I-(\theta+\beta)} - \frac{g\,(I-(\theta+\beta))}{g\,(I-(\theta+\beta))}\right]$$

$$T_{escape} = 2\tau \ln\left(\frac{g}{I-(\theta+\beta)} - 1\right) \tag{51}$$

⋆ **Regime 4:** $\frac{I-(\theta-\beta)}{g} < 0 < 1 < \frac{I-\theta}{g}$

In the fourth regime, as shown in Figure 12, the range of values defining the slow variables is defined within the values belonging to the jumping points. Moreover, the relationships between the parameters satisfy $I + \beta < \theta$ and $\theta \leq I - g$ by taking into account the limiting values for the jumping lines.

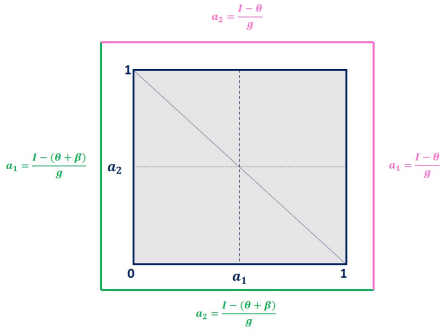

Figure 12: Graphical representation for **Regime 4**

Similarly to previous cases, an initial guess is made so that the system is initially started at $(u_1, u_2) = (1, 0)$, also implying that the slow variable associated to u_1 will increase whilst a_2 will decrease. Nevertheless, there will be no drastic switches in dynamics due to the fact that the unit square is contained inside the jumping values square. Thus, for $\frac{I-(\theta-\beta)}{g} < 0 < 1 < \frac{I-\theta}{g}$ no value of a_1 or a_2 will cross any of the jumping lines.

However, it is still possible to calculate the values that the fast variables will tend to by considering that u_1 and u_2 satisfy $u_i = H(I - \beta\, u_j - g\, a_i)$.

$$I - \beta\, u_2 - g\, a_1 = I - g\, a_1 \geq \theta \quad \forall a_1 \in (0, 1) \tag{52}$$

$$I - \beta\, u_1 - g\, a_2 = I - \beta - g\, a_2 \leq I - \beta < \theta \quad \forall a_2 \in (0,1) \tag{53}$$

Equations (52) and (53) respectively imply that $u_1 = H(I - \beta\, u_2 - g\, a_1) = 1$ and $u_2 = H(I - \beta\, u_1 - g\, a_2) = 0$. In other words, the values given to the fast variables in the initial guess will remain the same and the slow variables will behave such that $(a_1, a_2) \to (1, 0)$. Thus, we could conclude that this regime represents a **Winner-Take-All** mechanism; one population will be dominant over the other indefinitely, or unless an abrupt change of dynamics occurs [5].

Remark 3.5. In the case that $(u_1, u_2) = (0, 1)$ was taken as the initial guess instead, the same argument presented would follow. However, note that in that case, the Winner-Take-All regime would appear for $(u_1, u_2) = (0, 1)$.

⋆ **Regime 5:** $\frac{I-(\theta-\beta)}{g} < 0 < \frac{1}{2} < \frac{I-\theta}{g} < 1$

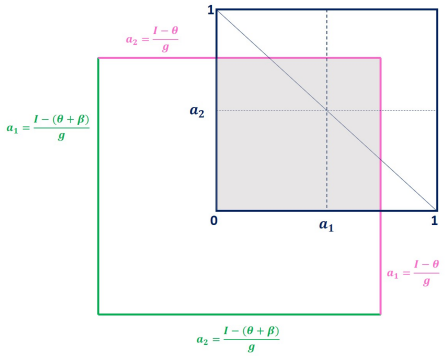

Figure 13: Graphical representation for **Regime 5**

Regime 5, as shown in Figure (13), is an oscillatory regime that crosses the main diagonal of the unit square of slow variables and it is defined for $\frac{I-(\theta-\beta)}{g} < 0 < \frac{1}{2} < \frac{I-\theta}{g} < 1$; i.e. $I - \beta < \theta$ and $2I - g > \theta$. For that reason, the discussion will follow very closely the argument presented in **Regime 3** and therefore, it will only highlight relevant results.

If $u_1 = 1, u_2 = 0$ are taken as initial values for the fast variables of the system, then the only possible jumping line that the slow variables could cross would be $a_1^* = \frac{I-\theta}{g}$ - see Figure 13. When the crossing occurs, u_1 will abruptly switch state and become inactivated and the value of u_2 after the jump will be defined by $u_2 = H(I - \beta\, u_1 - g\, a_2)$ and $a_2 = 1 - a_1^*$.

$$I - \beta\, u_1 - g\, a_2 = I - g\left(1 - \frac{I-\theta}{g}\right) = 2I - g - \theta > \theta \tag{54}$$

Equation (54) implies that just after the jump $u_2 = 1$, causing the fast variables to switch their active/inactive state. However, as $(u_1, u_2) = (0, 1)$ represent an unstable equilibrium point, the system

could continue to oscillate, still looking for another abrupt switch. Moreover, the slow variables a_1 and a_2 would then respectively decrease and increase giving rise to another possible crossing of the jumping lines. Therefore, the only jumping line that could be crossed again would be $a_2^* = \frac{I-\theta}{g}$, leading to an abrupt suppression of u_2 and activation of u_1 just after the jump.

Thus, we conclude that **Regime 5** models the oscillatory dynamics for the system; regulated by abrupt switchings of the states belonging to the fast variables when they cross the $\frac{I-\theta}{g}$ jumping lines. In other words, these particular dynamics exemplify a **release mechanism**.

Similarly to escape mechanisms, **release mechanisms** have an associated period for which they will occur, and it can be calculated by integrating one of the equations belonging to the slow variables with respect to time. In particular, for discussion purposes, we have decided to model the release period using the equation associated to the slow variable a_1.

$$\tau \frac{da_1}{dt} = -a_1 + u_1 \quad \Rightarrow \quad \tau \frac{da_1}{dt} = -a_1 + 1 \tag{55}$$

$$\int \frac{1}{1-a_1} da_1 = \int -\frac{1}{\tau} dt$$

$$\ln(1-a_1) = -\frac{1}{\tau} t + C$$

$$1 - a_1 = Ce^{-\frac{-t}{\tau}}$$

Again, similarly to **Regime 3**, any solution belonging to the slow variable a_1 is required to satisfy (55). For this reason, we considered the initial condition of the system to be of the form $1 - a_i$.

$$a_1(t) = 1 - (1-a_i)e^{-\frac{t}{\tau}}, \quad t \in \left(0, \frac{T}{2}\right) \tag{56}$$

Moreover, the period of oscillation can be computed by substituting $t = \frac{T}{2}$ into (56).

$$\frac{1-a_1}{1-a_i} = e^{-\frac{T}{2\tau}}$$

$$\ln\left(\frac{1-a_i}{1-a_1}\right) = \frac{T}{2\tau}$$

$$T = 2\tau \ln\left(\frac{1-a_i}{1-a_1}\right) \tag{57}$$

Finally, taking into account that there exists a release mechanism when the line $a_R = \frac{I-\theta}{g}$ is intersected by a_1^*, equation (57) can be rearranged to define the period of release, $T_{release}$. Recall that the value associated to a_1 just after the jump is $a_i = 1 - a_2^*$.

$$T = 2\tau \ln\left(\frac{1-1+a_2^*}{1-a_1^*}\right) = 2\tau \ln\left(\frac{a_2^*}{1-a_1^*}\right) = 2\tau \ln\left(\frac{I-\theta}{g} \cdot \frac{1}{1-\frac{I-\theta}{g}}\right) =$$

$$= 2\tau \ln\left(\frac{g}{g-I+\theta} - \frac{g-I+\theta}{g-I+\theta}\right)$$

$$T_{release} = 2\tau \ln\left(\frac{g}{g-I+\theta} - 1\right) \tag{58}$$

⋆ **Regime 6:** $\frac{I-(\theta-\beta)}{g} < 0 < \frac{I-\theta}{g} < \frac{1}{2}$

Figure 14 (left) graphically represents the area where the dynamics of the system occur. In this case the system will not undergo any oscillations, as the diagonal that models the oscillatory dynamics is not being crossed. The argument underlying the dynamics for this regime is very similar to the one discussed in **Regime 2**. For that reason, only important results will be highlighted.

Following previous arguments discussed, assume that initially the system is defined such that $(u_1, u_2) = (1, 0)$. If this occurs, the associated slow variables a_1, a_2 will respectively increase and decrease their values. Therefore, the only possible switch in dynamics will occur when crossing the jumping line for the u_1-nullcline; $a_1^* = \frac{I-\theta}{g}$. In this case, u_1 will be automatically suppressed and u_2 will be computed by setting $u_2 = H(I - \beta\, u_1 - g\, a_2)$ and $a_2 = 1 - a_1^*$.

$$I - \beta\, u_1 - g\, a_2 = I - g\left(1 - \frac{I-\theta}{g}\right) = 2I - \theta - g < \theta \quad \text{due to} \quad \frac{I-\theta}{g} < \frac{1}{2} \tag{59}$$

Equation (59) directly implies that $u_2 = H(I - \beta\, u_1 - g\, a_2) = 0$. Thus, both the system's fast and slow dynamics will be regulated by only one attractor point; $(u_1, u_2) = (0, 0)$ and $(a_1, a_2) = (0, 0)$ respectively.

⋆ **Regime 7:** $\frac{I-(\theta-\beta)}{g} < \frac{I-\theta}{g} < 0$

Similarly to **Regime 1**, the square of jumping values in **Regime 7** lies outside the unit square and thus, $\frac{I-(\theta-\beta)}{g} < \frac{I-\theta}{g} < (a_1, a_2)$ - see Figure 14 (right). Again, rearranging the limiting inequalities that define the expressions for the jumping points gives that $I - \beta < \theta$ and $I < \theta$. Moreover,

$$I - \beta\, u_j - g\, a_i < I < \theta \tag{60}$$

Finally, considering that $u_i = H(I - \beta\, u_j - g\, a_i)$ it follows that $(u_1, u_2) = (0, 0)$ and therefore, results imply that both populations will become inactive for any value of the slow variables.

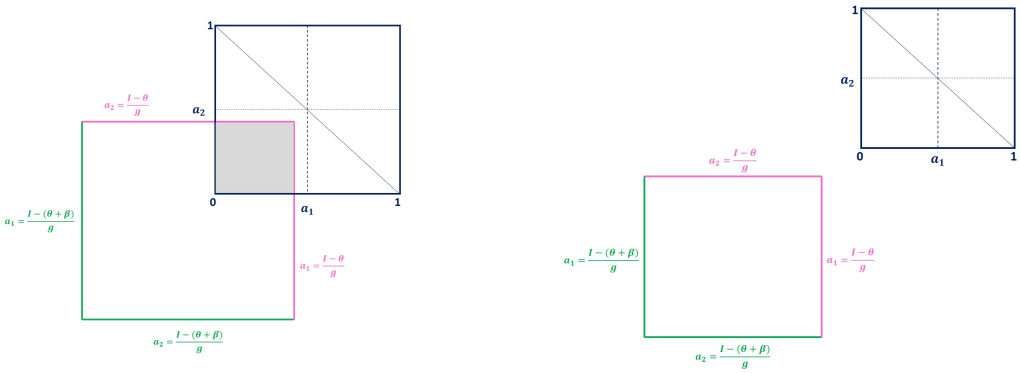

Figure 14: Graphical representation for **Regime 6** (left) and **Regime 7** (right)

3.3 Bifurcation diagrams and Levelt's propositions

This section of the thesis explores the mechanisms underlying oscillatory behaviours by analysing specific bifurcation diagrams and drawing relations with some of Levelt's propositions. In order to get a general overview on the dynamics that can possibly arise for different strengths of inhibition, a two-parameter diagram exploring the relationship between β and I was computed. Figure 15 shows that for inhibitory strengths lower than $\beta \approx 0.45$, the system will be on a stable state given any value of the input strength. On the other hand, bifurcations will begin to gradually appear for higher values of β; starting by the presence of oscillatory dynamics through a Supercritical Hopf bifurcation up to the establishment of a Winner-Take-All regime.

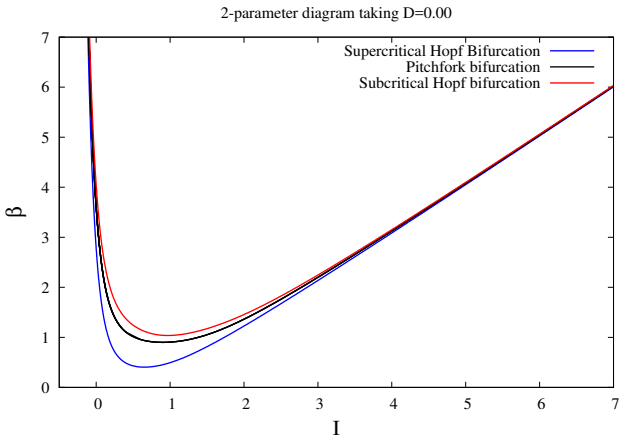

Figure 15: Two-parameter diagram setting $D = 0.00$

The bifurcation diagrams presented in the following discussions have been computed by setting the input strength I as the main parameter of the system. Moreover, in order to fully understand the oscillatory behaviours, two specific cases for the inhibition strength parameter, β, have been considered: $\beta = 1.1$ and $\beta = 0.75$. These values were chosen because Figure 15 shows that oscillatory dynamics could be expected for $\beta = 0.75$ and that Winner-Take-All behaviours could occur given $\beta = 1.1$.

Finally, note that in the following figures different coloured lines have been chosen to represent different type of dynamic phenomena. Red lines illustrate stable equilibria of the system whereas black lines represent unstable states. On the other hand, lines that are colored in green represent possible limit cycles that exist within the system.

1. Taking $\beta = 0.75$

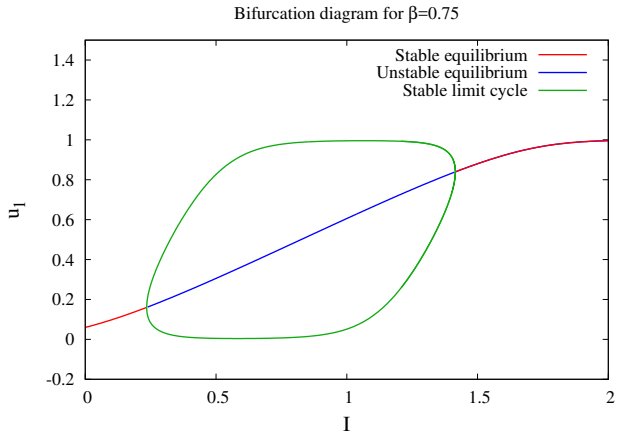

Figure 16: Bifurcation diagram with I as the main variable and setting $\beta = 0.75$

The bifurcation diagram illustrating the evolution of the fast variable u_1 with respect to the input strength I has been plotted in Figure 16 taking $\beta = 0.75$. Note that there exists a limit cycle for intermediate values of I, where perception alternates between the two populations governing the system. In other words, due to neuron populations continuously switching dominance, the system will oscillate until one of the populations becomes completely dominant.

Moreover, there exists two switching points that induce a change on the dynamics of the system. When $I \approx 0.2$, the stable equilibria transitions into a stable limit cycle through a Supercritical Hopf bifurcation. On the other hand, shortly after the oscillatory regime of the system, when I reaches $I \approx 1.6$, the stable limit cycles encounters another Supercritical Hopf bifurcation which immediately transforms the oscillatory dynamics into stable equilibria. These two bifurcation points illustrate the competitive behaviour of the model by differentiating two dominant stages from an oscillatory regime.

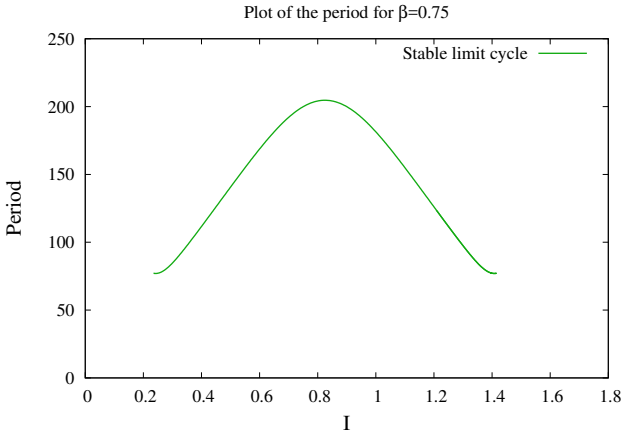

Figure 17: Plot of the period setting $\beta = 0.75$

Levelt's proposition (IV) - see Chapter 2 - will be used to further study and interpret the behaviour between the two populations of neurons and discuss the effect the input strength has with respect to the oscillatory regimes. Figure 17 shows the evolution that the period of oscillations corresponding to the above bifurcation diagram has with respect to I. It can be seen that there is no difference between the behaviour of both population of neurons; the graph is completely symmetric. Moreover, the increase on the input strength causes a decrease on the period of oscillations only for values $I > 0.8$, meaning that for these values of I the dominance time of each eyes' percepts also decreases. Thus, Levelt's proposition (IV) will only be satisfied for high values of I.

2. Taking $\beta = 1.1$

As it can be seen in Figure 18, the dynamical regime of the system changes for $\beta = 1.1$ and includes more oscillatory dynamics, as well as introducing a new bistability region.

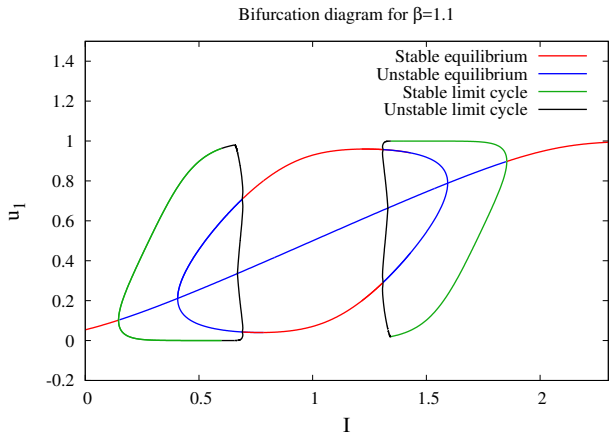

Figure 18: Bifurcation diagram with I as the main variable and setting $\beta = 1.1$

Taking a closer look to the bifurcation diagram, allows the reader to see that the oscillatory regime described for $\beta = 0.75$ in Figure 16 has been split into two sections, corresponding to low and high values of the input strength function I. On the other hand, for intermediate values of I, a new bistable regime has arose. The three regimes are connected through Hopf bifurcations and their transition is modelled by the change between unstable to stable equilibria, causing unstable limit cycles to appear. Moreover, two Pitchfork bifurcations have also appeared for $I \approx 0.45$ and $I \approx 1.5$.

The local dynamics of the bistability regime show that its stable equilibria is only associated to one of the percepts and therefore, it implies that the other image will be suppressed indefinitely. Thus, as the establishment of the regime would depend on the initial conditions of the system, we could conclude that the bistable regime represents a **Winner-Take-All behaviour**.

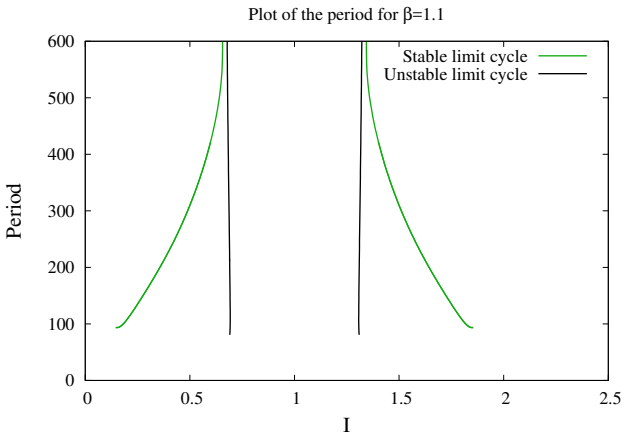

Figure 19: Plot of the period setting $\beta = 1.1$

Figure 19 illustrates the evolution of the period of oscillations with respect to the input strength. Similarly to the discussion associated to Figure 17, the fourth proposition that listed Levelt in 1965 will only be satisfied for the oscillatory regime that comes after the Winner-Take-All behaviour of the system - i.e. $I > 1.3$. Note that if I is defined for high values, an increase on its value would cause a decrease on the oscillations and therefore, promote the dynamics to tend to a stable state.

Comparing the dynamics illustrated on Figure 17 and Figure 19, it can be concluded that when the stability of the limit cycle and the equilibria change (i.e. for the values of I that are associated to the bifurcation points), the period will tend to infinity and it will acquire an asymptotic behaviour which will then be reflected in the form of abrupt changes in Figure 19. Moreover, it is important to remark that the period drastically increases for low values of I and later decreases for high values of the input strength. Finally, the figure also shows an intermediate stage of the plot for which the period is not represented and corresponds to the Winner-Take-All regime in Figure 18. In other words, Figure 19 shows that Winner-Take-All will be achieved through a release mechanism and it will terminate through an escape mechanism, represented by the second section of the stable limit cycle.

4. Visual attention as a recurrent excitatory input

We are interested in studying the effect of attention in models of bistable perception, that is, how does attention interact with incoming sensory information to determine what we perceive under ambiguous stimuli? As reported in the survey from Dieter et al. [6], this is a controverted issue in the literature except for one special instance of bistable perception: binocular rivalry. In this case, there are evidences that visual attention is required for alternations in perception when different stimuli are presented on each eye.

The entanglement of attention with binocular rivalry has been modeled by Li et al. in [9]. Due to the specificity of the problem (bistable perception is much more general than binocular rivalry), the model by Li et al. contains a level of detail not comparable to the previous models we have presented in this thesis. Indeed, the model contains 18 differential equations, including highly specialised pools of neurons such as monocular, binocular, attention and opponency ones. We have tried to analyse this model aiming to give a more complete description of the bifurcation diagram than the one in [9]. However, we have not been able to re-obtain the main results, even after a careful check of the code with the authors. For the sake of completeness, in Appendix A we have shown our study of the model whilst Appendix C provides the XPP code we implemented.

Nevertheless, fruitful discussion with part of the authors of [9] brought another way of studying attention to light: adding recurrence to the activity of both eyes, which can be modeled as a simple extension of Curtu et al. model studied in Chapter 3. The hypothesis hinges on the fact that attention is featured as a reinforcement of the current percept and thus, it induces the inclusion of a self-excitation term in both populations of the model. Here, we present the study of this extended version of Curtu et al.'s model, which is basically characterised by the addition of an attentional parameter called D.

4.1 The extended model

Following the introductory background presented in this Chapter, in order to analyse and discuss the effect of attention on binocular rivalry, we extended the model from Curtu et al. [5] by including a self-excitation term in each population of neurons, Du_j for $j = 1, 2$.

$$\begin{cases} \dot{u_1} = -u_1 + S(D\,u_1 - \beta\,u_2 - g\,a_1 + I) & (61) \\ \dot{u_2} = -u_2 + S(D\,u_2 - \beta\,u_1 - g\,a_2 + I) & (62) \\ \tau\dot{a_1} = -a_1 + u_1 & (63) \\ \tau\dot{a_2} = -a_2 + u_2 & (64) \end{cases}$$

Looking closely to the system of equations forming the extended model and focusing on the relationship between the excitatory recurrent term, D and the reciprocal inhibition parameter, β, we noticed that if the value of D increases then the value of the fast variable u_1 will augment too. If this occurs, then the negative effect of the reciprocal inhibition term $-\beta u_2$ in (62) will be higher and therefore, it will cause a decrease on the value of the fast variable u_2.

Psychophysically, this implies that the recurrent excitation applied to a population of neurons causes a faster inhibitory effect on the opposite population. In other words, the cross inhibition effect between both populations will be higher. Nevertheless, it is important to pinpoint that due to the fact that the excitatory recurrence term is applied to both populations at the same time, self-recurrent excitation (an increase on D) would be expected to influence a more sudden and faster change on the oscillatory dynamics.

Furthermore, in their research, Dieter et al. [6] argued that visual attention directly promotes the inhibitory effect and frequency of alternations between competing populations. In other words, research suggests that attention could have a positive effect on the oscillatory dynamics of the system by inducing dynamics to occur at a faster rate [6].

Taking into account the above observations and arguments, we decided that the analysis and discussion of attention in Curtu el al.'s model would start by exploring the variation on the relationship between the bifurcation parameters β and I for small values of D. Moreover, as the above paragraphs suggested, we also assumed that excitatory recurrence would trigger a change on the dynamics in the system. Thus, the following hypothesis were formulated

1. The bifurcation curves will move vertically when varying and reducing the inhibition parameter β.
2. Levelt's proposition (IV) will still be satisfied.
3. The introduction of a self-excitation term will reduce the range of values of I defined for the mechanisms of escape and release.

4.2 Diagrams and results obtained

Similarly to introductory sections in Chapter 3, in order to get a brief overview on the qualitative and quantitative dynamics of the system it would be necessary to analytically compute the critical points and their stability. Therefore, we want to solve $\dot{u_1} = \dot{u_2} = \dot{a_1} = \dot{a_2} = 0$. Thus,

$$\begin{cases} \dot{u_1} = -u_1 + S(D\,u_1 - \beta\,u_2 - g\,a_1 + I) = 0, \\ \dot{u_2} = -u_2 + S(D\,u_2 - \beta\,u_1 - g\,a_2 + I) = 0, \\ \tau\dot{a_1} = -a_1 + u_1 = 0, \\ \tau\dot{a_2} = -a_2 + u_2 = 0. \end{cases} \Rightarrow \quad \begin{cases} u_1 = S(D\,u_1 - \beta\,u_2 - g\,a_1 + I), \\ u_2 = S(D\,u_2 - \beta\,u_1 - g\,a_2 + I), \\ a_1 = u_1, \\ a_2 = u_2. \end{cases}$$

It is easy to see that the equilibrium points representing this system need to satisfy that $u_i = a_i$ for $i = 1, 2$ and thus, this implication reduces the initial system to

$$\begin{cases} u_1 = S(\,(D\ - g\,)a_1 - \beta\,u_2 + I), & (65) \\ u_2 = S(\,(D\ - g\,)a_2 - \beta\,u_1 + I). & (66) \end{cases}$$

Moreover, the extended model considers that both populations have the same self-excitation, i.e. the same value of D is applied to both. Then, if we define $g' := g - D$, equations (65) and (66) will reduce to

$$\begin{cases} u_1 = S(g' a_1 - \beta u_2 + I), & (67) \\ u_2 = S(g' a_2 - \beta u_1 + I). & (68) \end{cases}$$

It is easy to see that (67) and (68) have the exact same form as (11) and (12). Thus, the new extended model will satisfy the quantitative and qualitative analysis, as well as the mechanisms of release and escape, discussed in Chapter 3 for the binocular rivalry model of Curtu et al.

On the other hand, the relationship between the bifurcation parameters once a self-excitation term is introduced in the model was explored by computing two-parameter diagrams as well as bifurcation diagrams given specific values of D and β. The remaining of the section will present the results obtained and discuss the release and escape mechanisms for the model.

As an aside note, it is important to remark that the aim of the present study is to provide with an overview of the effect of attention in binocular rivalry. For that reason, and due to the complexity that arises for bigger values of D, as shown in Figure 20, we have only considered values for $D < 0.8$.

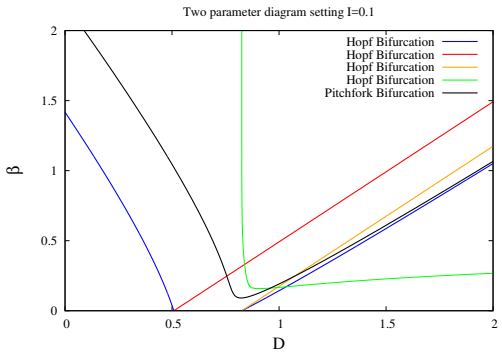

Figure 20: Two-parameter diagram setting $I = 0.1$

A general overview of the effect of the self-excitation parameter on the system was obtained by comparing the results shown in Figure 15 with new ones found for a varying value of D. For that, two-parameter diagrams exploring the relationship between the inhibition parameter β and the external input I were computed for three different and increasing values of D - see Figure 21.

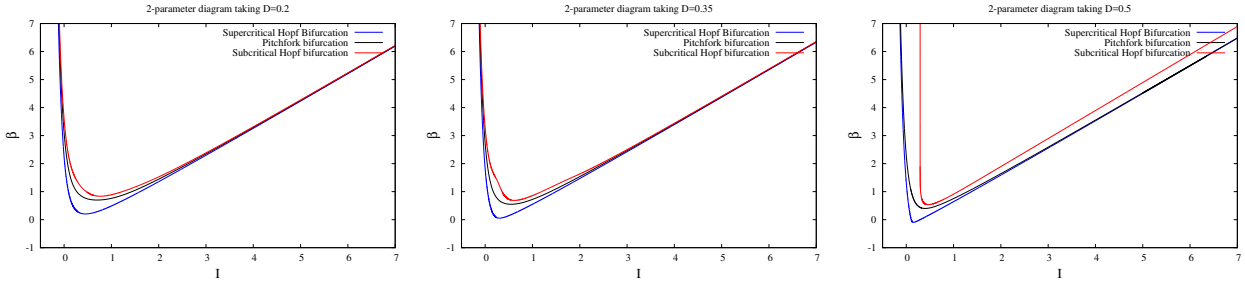

Figure 21: Two-parameter diagram setting, from left to right, $D = 0.2$, $D = 0.35$ and $D = 0.5$.

Figure 21 shows that, as the value of D increases, the bifurcation curves move downwards and start appearing for lower values of β. Therefore, the result suggests that $D > 0$ introduces the systems defined for small values of β to broader ranges of dynamics. Furthermore, the bifurcation curves represented in the three diagrams lead to think that for high values of the self-excitation parameter, oscillatory dynamics will occur for lower ranges of I, giving more presence to Winner-Take-All behaviours. Finally, it is also noticeable that, although different dynamics are more accessible for lower values of the inhibitory parameter β, bifurcation behaviours will occur for smaller ranges of the external input I. This fact will promote an increase on the frequency of alternations which, at the same time, can influence an earlier achievement of a stable state.

For that reason, we felt necessary to have a closer look to the relationship between the external input strength, I, applied to the system and the excitatory term, D, applied directly on the population of neurons. We decided to consider three different values for the inhibitory parameter in order to track the evolution of the relationship between the two parameters with respect to the bifurcation curves. Figure 22 shows three different I vs. D diagrams computed for $\beta = 0.35$, $\beta = 0.75$ and $\beta = 1.1$.

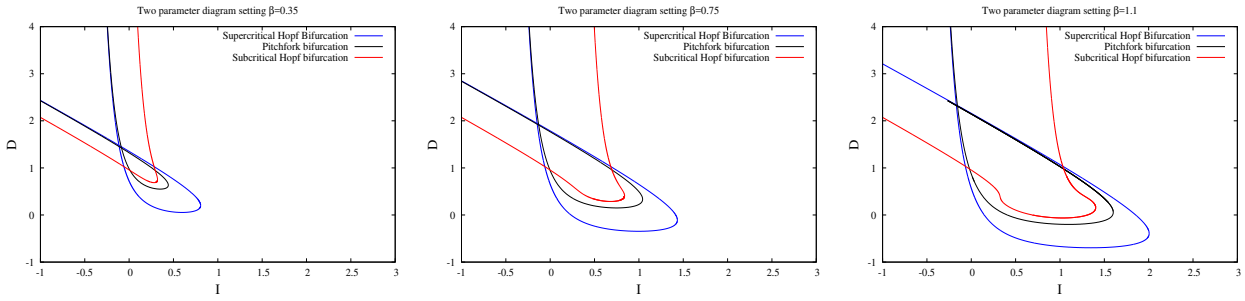

Figure 22: Two-parameter diagram setting, from left to right, $\beta = 0.35$, $\beta = 0.75$ and $\beta = 1.1$.

Firstly, it is interesting to notice that the three relationships plotted for different values of β seem to follow a similar fashion, inducing to think that similar bifurcation dynamics will be accessible for any system no matter their inhibitory strengths. Moreover, the three diagrams show that there exists a direct relationship between the appearance of a range of bifurcation dynamics and the increase on the value of D, when I is considered to be fixed.

Into some extent, the results shown in Figure 22 give more strength to the conclusions and implications drawn by analysing Figure 21. When self-excitation on the neurons, i.e. visual attention, increases, com-

petitive behaviours become more complex and populations are more prompt to reach a Winner-Take-All state. In addition, the introduction of visual attention seems to have a catalysing effect on the alternating frequency of the dynamics; if more attention is applied whilst keeping the inhibitory term fixed, bifurcation dynamics will occur for shorter variations of I and they will tend to a stable state faster. Psychophysically, this would mean that attention promotes binocular rivalry processes, whilst inducing one competing population of neurons to reach a dominant state more easily and for lower external stimulations applied.

For example, Figure 23 shows the effect of self-excitation on neuron populations for $\beta = 0.35$. Recall that in the model of Curtu et al., there was no rivalry or oscillatory dynamics between competing stimuli for $\beta = 0.35$. For that reason, it is interesting to see that when the value of D is increased, keeping the strength of inhibition fixed, there is a sudden appearance of oscillatory dynamics on the system, where stimuli start to compete for dominance, implying that a binocular rivalry process has been *activated*.

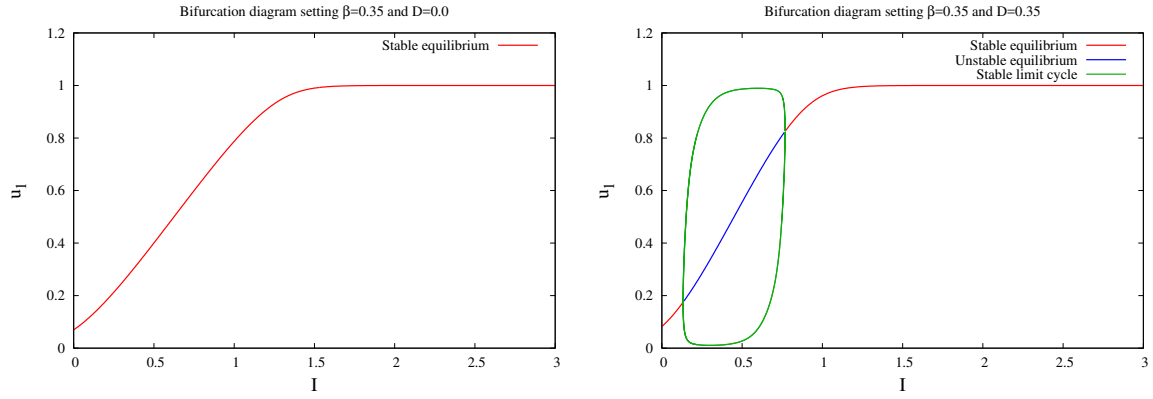

Figure 23: Bifurcation diagram setting $\beta = 0.35$ for $D = 0$ and $D = 0.35$, respectively.

A similar experiment was conducted for $\beta = 0.75$ and $\beta = 1.1$. On the one hand, while increasing the amount of self-excitation in neurons promoted a more varied but faster bifurcation dynamics for $\beta = 0.75$ - see Figure 24, attention had a different implication in situations where a stronger inhibition was exerted on the system, as shown in Figure 25.

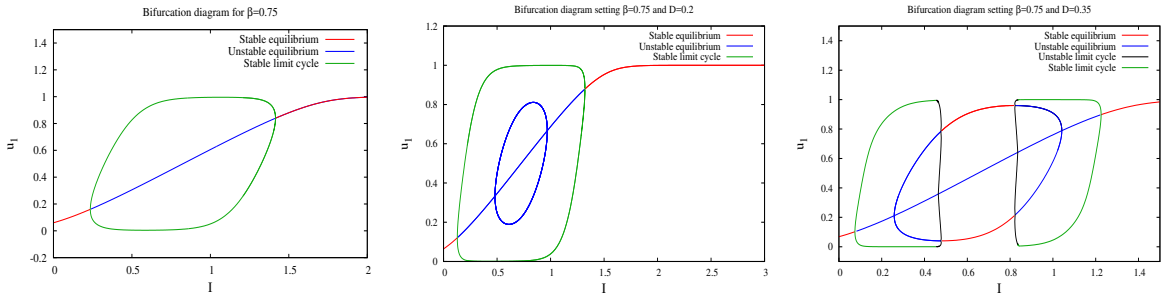

Figure 24: Bifurcation diagram setting $\beta = 0.75$ and for, from left to right, $D = 0$, $D = 0.2$ and $D = 0.35$

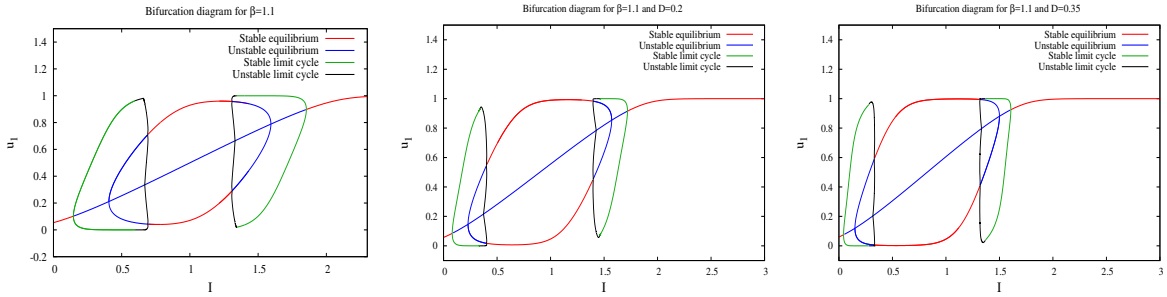

Figure 25: Bifurcation diagram setting $\beta = 1.1$ and for, from left to right, $D = 0$, $D = 0.2$ and $D = 0.35$

Both cases support the idea that attention increases the alternation rate between bifurcation dynamics and therefore, lower values of the external inputs will be sufficient to achieve similar dynamical behaviours. Nevertheless, Figure 25 also shows that, in the cases where Winner-Take-All behaviours were already achieved without attention, the application of self excitation to neurons causes oscillatory dynamics to happen faster and therefore, Winner-Take-All regimes tend to occur for larger ranges of I. Thus, this fact could also have an effect on the release and escape mechanisms of the system.

In order to check this assertion, diagrams of the period of oscillations setting $\beta = 0.75$ and $\beta = 1.1$ were plotted for the same three values of self-excitation, $D = 0$, $D = 0.2$ and $D = 0.35$.

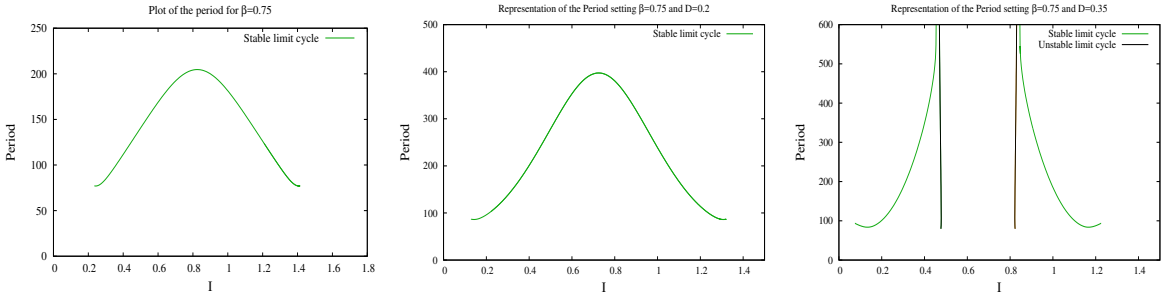

Figure 26: Diagram representing the period setting $\beta = 0.75$ for, from left to right, $D = 0$, $D = 0.2$ and $D = 0.35$.

Firstly, Figure 26 gives an overview of the evolution of the period under the effect of D. Results show that attention helps populations reach higher values of the period for smaller input strengths. Moreover, as it was discussed in Figure 24, increasing D also induces the appearance of release and escape mechanisms. In this particular case, for $\beta = 0.75$ and $D = 0.35$, there exists a release mechanism that occurs for $I \approx (0.1, 0.5)$, as well as an escape mechanism for $I \approx (0.85, 1.25)$. The region in between represents a Winner-Take-All behaviour, exemplified by the period asymptotically tending to infinity when $I \approx (0.5, 0.85)$.

It is also interesting to note that, although Levelt's fourth proposition is only satisfied for high values of I in the three cases, increasing self-excitation on neurons affects the extent in which escape and release mechanisms can occur. In other words, the appearance of Winner-Take-All regimes imply that release and

escape mechanisms will occur for high values of D, whereas for $D = 0$ and $D = 0.2$ oscillations will not lead to these type of mechanisms.

Finally, it is easy to see that for $\beta = 1.1$ the form of the graph of the period of oscillations remains the same, supporting the hypothesis that release and escape mechanisms stay even varying D and high inhibition strengths - see Figure 27. On the other hand, the ranges of I for which oscillatory dynamics occur become smaller, also reducing the possible values of I for which they can happen. Results show that this is due to larger Winner-Take-All regimes appearing. Nevertheless, in all three cases Levelt's proposition (IV) is only satisfied for the ranges in which the escape mechanisms occurs.

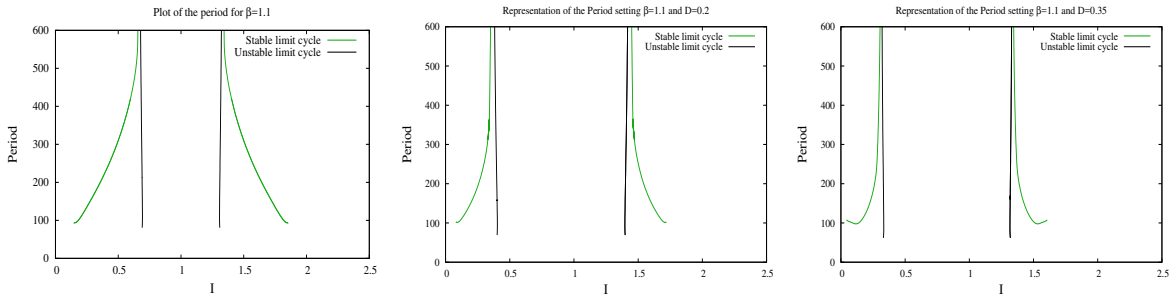

Figure 27: Diagram representing the period setting $\beta = 1.1$ for, from left to right, $D = 0$, $D = 0.2$ and $D = 0.35$.

5. Conclusion

This Master thesis aimed to discuss the influence and effects that visual attention has in binocular rivalry processes. For that, attention was modelled as a recurrent excitatory parameter applied on neuron populations and it was added to the original model of Curtu et al. that did not consider attention as an external factor. Moreover, following past research on the topic, it was also hypothesised that the introduction of attention into the system would promote the achievement of more bifurcation dynamics for lower inhibition strengths, still satisfying Levelt's proposition (IV) and mechanisms such as release and escape. Results were computed using the software *XXPAUT*, due to its focus on the representation of bifurcation diagrams, to illustrate different systems' dynamics.

Following the introductory background presented in Chapter 2, the stability analysis of the initial model of Curtu et al. (2008) gave the opportunity to introduce and discuss more in depth mechanisms such as release, escape and Winner-Take-All behaviours that occur on the alternations of dynamics. Moreover, bifurcation diagrams were plotted to discuss the implication and application of Levelt's proposition (IV) within the system; concluding that when release and escape mechanisms occur, proposition (IV) is not satisfied for the whole period but only in the area that belongs to the escape mechanism. Moreover, Chapter 3 has been key to understand the mechanisms and behaviours behind the extended model considered in the last chapter of the thesis, in which the effects of visual attention have been explored - see Chapter 4. For starters, it was interesting to realise that, due to both populations of neurons receiving the same recurrent excitation, the new system satisfied the same qualitative and quantitative dynamics that the initial model. Thus, we concluded that results highlighted in Chapter 3 were also applicable to the analysis in Chapter 4.

On the other hand, from the diagrams computed in Chapter 3 and 4 we were able to see that, as recent research suggested - see [6] -, attention had a catalyst effect on dynamic behaviours by promoting bifurcation dynamics on low inhibitory cases and inducing faster alternations between the dynamics of systems that considered higher values of β. We also noticed that attention positively affected Winner-Take-All behaviours, allowing them to appear for larger ranges of I. Furthermore, we noticed that the range of values of I for which the period was defined in some of the diagrams became narrower if $D > 0$, yet at the same time the diagram showed that higher values for the period were reached if attention was being considered. This finding supported the argument that suggested that one of the main effects of attention is linked to the frequency of alternations in dynamics. Finally, as initially guessed, we also showed that Levelt's proposition (IV), which was satisfied in the original model, was still satisfied in the extended model, but only for smaller ranges of the input strength I.

Overall, findings show that the main effects of attention in this particular binocular rivalry model follow a similar line to conclusions drawn in previous research papers conducted around the topic. Attention, as a form of self-excitatory input on neurons, seems to benefit the appearance of bifurcation dynamics, as well as making their period of oscillation shorter. In other words, the impression is that visual attention applied equally to both eyes preserves the general properties that would belong to same model if this factor was missing.

Further research could explore the effect of attention in situations where neurons had different self-excitatory inputs by considering one stimulus to be more prompt to be viewed than the other. Moreover, future contributions could also follow a similar structure to Curtu et al.'s analysis to quantitatively analyse

the mechanisms of release and escape for the extended model presented in this thesis. Hence or otherwise, it would also be interesting to fully understand the mechanisms and bifurcation dynamics behind Li et al.'s model as their way of understanding attention process could represent an inflection point on how visual attention is understood. On the same wavelength, another extension of Li et al.'s research could consist on exploring the effect of attention and opponency contributions separately.

References

[1] D. Alais and R. Blake. Binocular rivalry and perceptual ambiguity. In Johan Wagemans, editor, *The Oxford Handbook of Perceptual Organization*. Oxford University Press, 2015. Accessed through "`http://www.gestaltrevision.be/pdfs/oxford/Alais&Blake-Binocular_rivalry_and_perceptual_ambiguity.pdf`" in 08/04/2019.

[2] R. Blake. A neural theory of binocular rivalry. *Psychological Review*, 96(1):145 – 167, 1989.

[3] J.W. Brascamp, P.C Klink, and with a contribution from W.J.M Levelt. The 'laws' of binocular rivalry: 50 years of levelt's propositions. *Vision Research*, 109:20 – 37, 2015.

[4] R. Curtu. Singular hopf bifurcations and mixed-mode oscillations in a two-cell inhibitory neural network. *Physica D*, 239:504 – 514, 2010.

[5] R. Curtu, A. Shpiro, N. Rubin, and J. Rinzel. Mechanisms for frequency control in neuronal competition models. *Journal of Applied Dynamical Systems*, 7(2):609 – 649, 2008.

[6] K. Dieter, J. Brascamp, D. Tadin, and R. Blake. Does visual attention drive the dynamics of bistable perception? *Attention Perception Psychophysiology*, 78:1861 – 1873, 2016.

[7] P. García Rodríguez. *Noise-induced reversals in bistable visual perception*. PhD thesis, UPC - Departament de Matemàtica Aplicada I, 2012. Centre de Recerca Matemàtica.

[8] C. Laing and C. Chow. A spiking neuron model for binocular rivalry. *Journal of Computational Neuroscience*, 12:29 – 53, 2002.

[9] H. Li, J. Rankin, J. Rinzel, M. Carrasco, and D. Heeger. Attention model of binocular rivalry. *PNAS*, 114(30):192 – 201, 2017.

[10] N. Logothetis, D. Leopold, and D. Sheinberg. What is rivalling during binocular rivalry? *Letters to Nature*, 380:621 – 624, 1996.

[11] P. Mamassian and R. Goutcher. Temporal dynamics in bistable perception. *Journal of Vision*, 5:361 – 375, 2005.

[12] R. Moreno-Bote, J. Rinzel, and N. Rubin. Noise-induced alternations in an attractor network model of perceptual bistability. *Journal Neurophysiology*, 98:1125 – 1139, 2007.

[13] G. Rodríguez Martínez and H. Castillo Parra. Bistable perception: neural bases and usefulness in psychological research. *International Journal of Psychological Research*, 11:63 – 76, 2018.

[14] H.R. Wilson. Computational evidence for a rivalry hierarchy in vision. *PNAS*, 100:14499 – 14503, 2003.

Appendices

A. Li et al. (2017)'s attention model

A.1 General overview of the model

Li et al.'s (2017) model considered that in binocular rivalry two processes regulated competition; attention and inhibition between neurons [9]. It is important to recall that, as introduced in earlier sections of the thesis, the word attention here refers to visual attention. Furthermore, Li et al.'s attention model considered that three different groups of neurons took part in the rivalling process [9]. They divided them depending on their properties, interrelationships and the activities that they were subjected to within the neuron model [9].

The first group of neurons is referred in the model as *Sensory Representation* and considers the activity of three populations [9]. Two monocular populations of neurons are associated to the left eye and to the right eye, respectively. On the other hand, the third is linked to a binocular population of neurons. *Attentional modulation*, the second class of neurons, is only represented by a population of attention neurons, whereas *Mutual inhibition* illustrates the behaviour of two populations of opponency neurons that regulate the inhibition between right-eye and left-eye neurons and left-eye and right-eye neurons, respectively [9]. Thus, it could be concluded that while one of the groups is responsible for the analysis and response of the visual inputs that are received, the others model visual attention between stimuli and inhibition between competing percepts, respectively [9].

Figure 28, quoted from [9], illustrates the structure of the attention model of Li et al. (2017). The figure has been divided in three different sections, differentiating the relationships between neurons within the general model and neurons that influence processes such as attention and inhibition. In addition, each population is formed of two neurons which have a specific orientation associated to them. This model considers that the orientation of neurons within the same population must be different and orthogonal to each other [9].

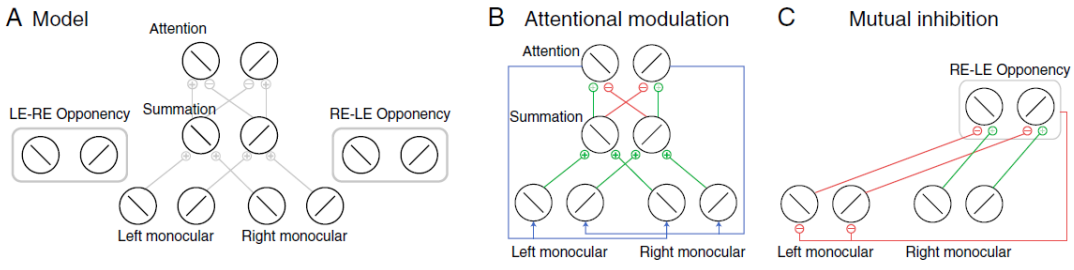

Figure 28: Li et al.'s model structure [9]

Figure 28A shows a general overview of the model's structure. Green lines represent excitation to and from neurons with the same orientation, whereas red lines represent suppressive inputs that come from neurons that have opposite orientations. Figures 28B and 28C look more closely to the mechanisms behind attention and inhibition between neurons.

Firstly, in Figure 28B, attentional modulation is modelled such that monocular neurons provide an excitatory input to binocular neurons with the same orthogonal orientation. At the same time, if we think of the model as being structured in layers, the process will be repeated again for attention neurons. On the other hand, the diagram establishes that attention can be inhibited by binocular neurons with opposite orientations, yet there is no suppressive relationship set between monocular and binocular neurons. Finally, blue lines represent attention gain factors, which are used to model the excitatory drive of monocular neurons and whose value depends on the response that attention neurons with the same orientation have [9].

Mathematically, the model only considers one population of two attention neurons which have a different orientation each, (R_{A1}, R_{A2}). τ_a is the time constant associated to this type of neurons and σ_A is the suppression constant [9]. Neural responses are modelled so that the activity of attention neurons can be suppressed by increasing the attention of the competing orientation, (71). This is modelled through a half-wave rectification function, $[]_+$, which only affects the value of the function when it becomes negative as any negative result will be set to zero.

$$\tau_a \frac{d}{dt} R_{A1} = -R_{A1} + \frac{E_{A1}}{S_A + \sigma_A^n} \tag{69}$$

$$E_{A1} = \text{sgn}\,(R_{B1} - R_{B2})\,(R_{B1} - R_{B2})^n \tag{70}$$

$$S_A = \sum_{k=1,2} [E_{Ak}]_+ \tag{71}$$

The excitatory drive of attention neurons - Eq.(70) - depends on the input response of binocular neurons (R_{B1}, R_{B2}) which strongly suggests that the alternations between binocular neurons will influence the response produced by attention neurons.

Moreover, the neural response of binocular neurons, (R_{B1}, R_{B2}), can be modelled considering, as discussed, excitatory and suppressive drives - (73),(74) -, as well as adaptation factors, (75). In the following equations, τ_s, τ_h, are the time parameters associated to binocular neurons and the adaptation process, respectively. Furthermore, w_h represents the weight of adaptation, and σ is the suppression parameter that takes different values depending on the type of neurons that are being modelled.

$$\tau_s \frac{d}{dt} R_{B1} = -R_{B1} + \frac{E_{B1}}{S_{B1} + H_{B1}^n + \sigma^n} \tag{72}$$

$$E_{B1} = (R_{L1} + R_{R1})^n \tag{73}$$

$$S_{B1} = E_{B1} \tag{74}$$

$$\tau_h \frac{d}{dt} H_{B1} = -H_{B1} + w_h R_{B1} \tag{75}$$

As previously introduced, the excitatory drive of binocular neurons (equation (73)) directly depends on the neural responses of monocular neurons that belong to different populations but have the same orientation. In particular, note that the suppressive drive for binocular neurons, S_{B1} has the same expression as their excitatory drive E_{B1}.

On the other hand, the general equation for monocular neurons (76) models the response that each monocular neuron associated to a specific eye and a specific orientation has over a time frame, $(R_{L1}, R_{L2}, R_{R1}, R_{R2})$. In the following system of equations, τ_s and τ_h are time constants; σ is a suppression parameter; w_o, w_a, w_h represent the weights of inhibition, attention and adaptation, respectively; D is the input strength and α is a given scaling factor [9].

$$\tau_s \frac{d}{dt} R_{L1} = -R_{L1} + \frac{\alpha E_{L1}}{S_m + H_{L1}^n + \sigma^n} \tag{76}$$

$$E_{L1} = [D_{L1}^n - w_o O_R]_+ [1 + w_a R_{A1}]_+ \tag{77}$$

$$S_m = \sum_{k=1,2} E_{Lk} + \sum_{k=1,2} E_{Rk} \tag{78}$$

$$\tau_h \frac{d}{dt} H_{L1} = -H_{L1} + w_h R_{L1} \tag{79}$$

Moreover, factors such as excitation, suppression and adaptation have also been considered to influence the response of a monocular neuron [9] and therefore, they have been included in the model - see equations (77),(78),(79). $[1 + w_a R_{A1}]_+$ represents the attention impact on the neurons, which can differ in each case depending on the individual response of the attention neuron [9]. On the other hand, the factor $[D_{L1}^n - w_o O_R]_+$ illustrates the inhibition belonging to the competing eye derived by the responses of the opponency neurons that are being subtracted from the input strength.

Finally, Figure 28C illustrates the neural mechanisms behind inhibition regulated by opponency neurons. Recall that the model considers two populations of opponency neurons that depend on the type of neurons that are being suppressed [9]. For example, in the case that Right-Eye-to-Left-Eye (RE-LE) neurons are modelled, Right-Eye (RE) neurons send the excitatory input to the opponency neurons, whereas Left-Eye (LE) neurons provide them with the suppressive input. Shortly after, RE-LE neurons compute the difference in response between these two types of neurons and they send the corresponding result as a form of inhibitory input to LE monocular neurons.

Thus, opponency neurons characterise themselves by illustrating the inhibitory relationship between the two eyes [9]. The model considers the neural response of two populations of opponency neurons formed by two neurons with different orientations each, $(R_{OR1}, R_{OR2}, R_{OL1}, R_{OL2})$. The equations forwarded in this section represent the inhibitory response of Right-to-Left opponency neurons.

$$\tau_o \frac{d}{dt} R_{OR1} = -R_{OR1} + \frac{E_{OR1}}{S_{OR} + \sigma^n} \tag{80}$$

The excitatory drive of opponency neurons (81) is always computed with respect to the neural responses of monocular neurons, yet in this case right and left monocular neurons that have the same orientation are required [9].

$$E_{OR1} = [R_{R1} - R_{L1}]^n_+ \tag{81}$$

$$S_{OR} = \sum_{k=1,2} E_{ORk} \tag{82}$$

Lastly, recall that opponency neurons will have an inhibitory effect on some of the other neurons - Eq.(83). O_R, for example, acumulates the neural responses of the two opponency neurons that belong to the same population. This factor will be later subtracted from the excitatory drive of monocular neurons modelling the process of inhibition between competing eyes [9].

$$O_R = \sum_{k=1,2} R_{ORk} \tag{83}$$

To sum up, this section on the appendix aimed to give a general overview of the model and describe the general equations that illustrate the behaviour of the different types of neurons. For that reason, only one neuron per type has been used each time to illustrate each process.

A.2 Results obtained

This section presents two graphical results that we obtained for the present model. Although the results that we have obtained do not correspond to the conclusions and diagrams proposed in Li et al.'s article - see [9], we have decided to present them in the appendices for illustrative purposes.

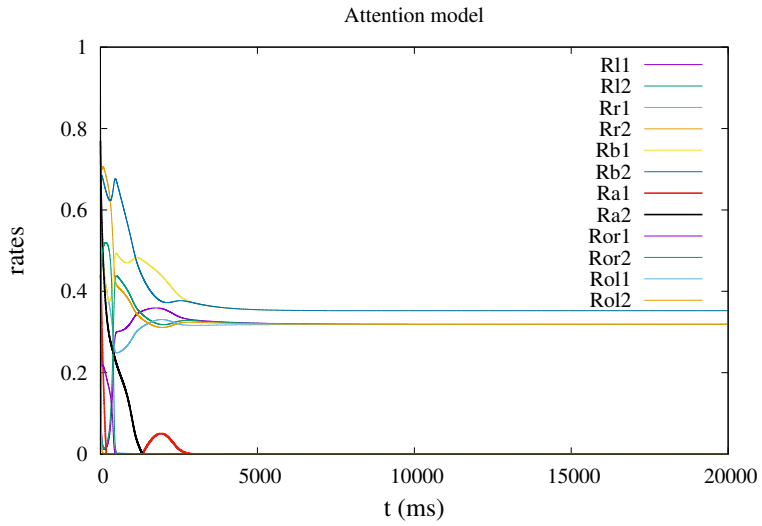

Figure 29: Evolution of the variables of the model with respect to time.

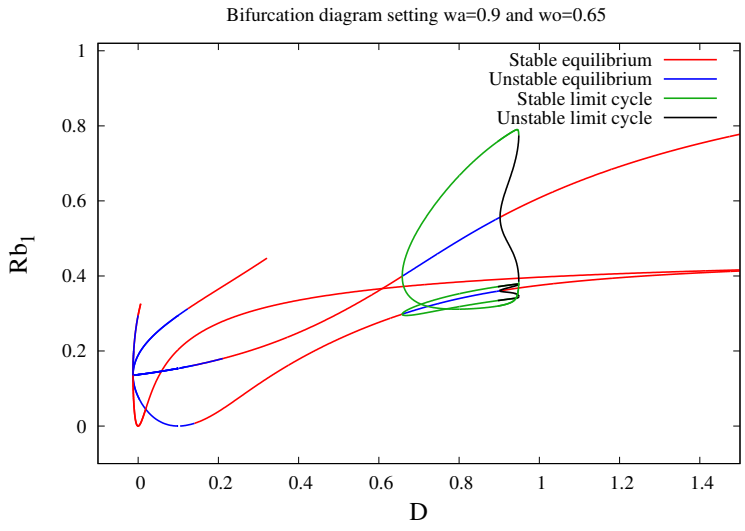

Figure 30: Bifurcation diagram setting $wa = 0.9$ and $wo = 0.65$.

B. An introduction to the slow variables' manifold for the sigmoid gain function

This Appendix section aims to give a brief analysis into the derivation of the manifold of slow variables where release and escape dynamics of the original system with sigmoid gain function occur. In order to derive the expression for the slow manifold, we need to consider a slow time parameter s say, so that it represents an inverse expression of the original time constant τ; i.e. $s = \frac{1}{\tau}t = \epsilon t$. From now on, time derivatives will be taken with respect to s in order to characterise solutions within the slow manifold. Rewriting (7), (8), (9) and (10) with respect to the slow time derivatives gives the following system.

$$\begin{cases} \epsilon \dfrac{du_1}{ds} = -u_1 + S(I - \beta\, u_2 - g\, a_1) \\ \epsilon \dfrac{du_2}{ds} = -u_2 + S(I - \beta\, u_1 - g\, a_2) \\ \dfrac{da_1}{ds} = -a_1 + u_1 \\ \dfrac{da_2}{ds} = -a_2 + u_2 \end{cases}$$

From Curtu et al.'s research - see [5] - we know that if $\epsilon = 0$, the solution for the present model will always belong to the slow manifold. Thus, any solutions satisfying

$$-u_1 + S(I - \beta\, u_2 - g\, a_1) = 0 \tag{84}$$

and

$$-u_2 + S(I - \beta\, u_1 - g\, a_2) = 0 \tag{85}$$

will belong to the region that we are seeking. In addition, after rearranging and simplifying (84) and (85) we can find the expressions belonging to the fast and slow variables within the slow manifolds. First, we can start by respectively writing u_1 and u_2 as

$$u_1 = S(I - \beta\, u_2 - g\, a_1) \tag{86}$$

and

$$u_2 = S(I - \beta\, u_1 - g\, a_2) \tag{87}$$

Multiplying both sides of the equations by the inverse of the sigmoid funcion $F(u)$ gives, in the same order,

$$F(u_1) = I - \beta\, u_2 - g\, a_1 \tag{88}$$

and

$$F(u_2) = I - \beta\, u_1 - g\, a_2 \tag{89}$$

Therefore, we could argue that solutions associated to the slow variables a_1, a_2 could be expressed with respect to the values that the fast variables u_1, u_2 take.

Proposition B.1. *Let Σ be a surface that represents the dynamics associated to the solutions that belong to the slow variables a_1 and a_2. Then, if a_1 is defined with respect to a_2 and u_1 and the relationships between variables are considered in the slow manifold, one can define Σ as*

$$\Sigma = \{(u_1, u_2, a_1, a_2) : u_1, u_2 \in (0,1), a_1, a_2 \in \Re, \text{ and}$$
$$u_2 = S(I - \beta\, u_1 - g\, a_2), a_1 = \frac{1}{g}\left[I - F(u_1) - \beta S(I - \beta\, u_1 - g\, a_2)\right]\} \tag{90}$$

Proof. Firstly, rearranging (88) for a_1 gives the following expression with respect to the two fast variables.

$$F(u_1) = I - \beta\, u_2 - g\, a_1 \;\Rightarrow\; g\, a_1 = I - \beta\, u_2 - F(u_1)$$

After substituting u_2 for the equivalent expression in (87) we obtain

$$g\, a_1 = I - F(u_1) - \beta S(I - \beta\, u_1 - g\, a_2) \;\Rightarrow\; a_1 = \frac{1}{g}\left[I - F(u_1) - \beta S(I - \beta\, u_1 - g\, a_2)\right]$$

Similarly for a_2,

$$F(u_2) = I - \beta\, u_1 - g\, a_2 \;\Rightarrow\; g\, a_2 = I - \beta\, u_1 - F(u_2) \tag{91}$$

Thus, if the expression of u_1 satisfying (86) is substituted into (91), the expression for the solutions belonging to the slow variable a_2 will be found.

$$g\, a_2 = I - F(u_2) - \beta S(I - \beta\, u_2 - g\, a_1) \;\Rightarrow\; a_2 = \frac{1}{g}\left[I - F(u_2) - \beta S(I - \beta\, u_2 - g\, a_1)\right]$$

Finally, if u_1 and u_2 represent competing populations, then the state associated to the fast variables will continuously change from active to inactive, mathematically implying that $(u_1, u_2) \in (0,1)$. On the other hand, the slow variables a_1, a_2 could take any real value.

□

Applying proposition B.1 to the original model provides us with an alternative manner of analysing neuron dynamics on the plane of the slow variables [5]. Reducing the original system to the following system of equations for $(\tilde{u_1},\ \tilde{u_2},\ a_1,\ a_2) \in \Sigma$ gives

$$\begin{cases} \dfrac{da_1}{ds} = -a_1 + \tilde{u_1}(a_1, a_2) & (92) \\ \dfrac{da_2}{ds} = -a_2 + \tilde{u_2}(a_1, a_2) & (93) \end{cases}$$

Similarly to the procedure and mathematical reasoning followed during the analysis of the Heaviside function case in section 3.2.1, computing the nullclines of the new system is a first step for describing the equilibrium points and oscillatory dynamics of neurons.

- a_1-**nullcline (N_1):** $\frac{da_1}{ds} = 0$. Therefore, $a_1 = \tilde{u_1}(a_1, a_2)$.
- a_2-**nullcline (N_2):** $\frac{da_2}{ds} = 0$. Then $a_2 = \tilde{u_2}(a_1, a_2)$.

The a_1-nullcline represents a curve contained within Σ that illustrates the possible dynamics and equilibria of the variables a_1 and $\tilde{u_1}$ on the slow plane. Thus, the expression for this nullcline could be rewritten in more general terms, as well as with respect to Σ and the remaining associated variables.

On the one hand, recall that the nullclines associated to the slow variable a_1 and a_2 are respectively defined such that

$$a_1 = \tilde{u_1}(a_1, a_2) \tag{94}$$

$$a_2 = \tilde{u_2}(a_1, a_2) \tag{95}$$

In addition, consider $u_1 \approx \tilde{u_1} = S(I - \beta\, u_2 - g\, a_1)$. Therefore, the last mathematical equality, (94), can be written as $F(a_1) = I - \beta\, u_2 - g\, a_1$ which, rearranging it for u_2, gives that $u_2 = \frac{I - F(a_1) - g\, a_1}{\beta}$. Furthermore, from (89) and (94) we can derive an expression for the slow variable a_2 with respect to a_1 to ensure that this particular variable is contained within the curve belonging to $\frac{da_1}{ds} = 0$.

$$a_2 = \frac{I - \beta a_1 - F(u_2)}{g} = \frac{1}{g}\left[I - \beta a_1 - F\left(\frac{I - F(a_1) - g\, a_1}{\beta}\right)\right], \quad a_2 \in (\alpha_1, \alpha_2)$$

Thus, we can summarize the dynamics of the slow variable's a_1- nullcline with respect to Σ as follows

$$N_1 = \Bigg\{ (\tilde{u_1}, \tilde{u_2}, a_1, a_2) : \tilde{u_1} = a_1, \tilde{u_2} = S(I - \beta a_1 - g\, a_2(a_1)) \text{ and}$$

$$a_2 = \frac{1}{g}\left[I - \beta a_1 - F\left(\frac{I - F(a_1) - g\, a_1}{\beta} \right) \right], \quad a_2 \in (\alpha_1, \alpha_2) \text{ where } \alpha_1, \alpha_2 \in (0,1) \Bigg\} \tag{96}$$

Similarly, we can also express the a_2-nullcline - see (95) - with respect to the surface of slow variables Σ. Again, setting $u_2 \approx \tilde{u_2}$ and using the properties belonging to the fast variables u_1 and u_2, it is easy to see that $u_1 = \frac{I - F(a_2) - g\, a_2}{\beta}$ on this particular curve.

In addition, following a similar procedure to the ones discussed in previous calculations, $a_1 = \frac{I - \beta a_2 - F(u_1)}{g}$ represents a necessary condition for the slow variable a_2 to belong to the curve $\frac{da_2}{ds} = 0$. Finally, substituting (95) and (89) into the expression defining the slow variable a_1 gives

$$a_1 = \frac{1}{g}\left[I - \beta a_2 - F\left(\frac{I - F(a_2) - g\, a_2}{\beta} \right) \right], \quad a_1 \in (\alpha_1, \alpha_2)$$

Thus, we can finally express N_2 with respect to the surface of slow variables Σ.

$$N_2 = \Bigg\{ (\tilde{u_1}, \tilde{u_2}, a_1, a_2) : \tilde{u_2} = a_2, \tilde{u_1} = S(I - \beta a_2 - g\, a_1(a_2)) \text{ and}$$

$$a_1 = \frac{1}{g}\left[I - \beta a_2 - F\left(\frac{I - F(a_2) - g\, a_2}{\beta} \right) \right], \quad a_1 \in (\alpha_1, \alpha_2) \text{ where } \alpha_1, \alpha_2 \in (0,1) \Bigg\} \tag{97}$$

On the other hand, recall that it is also possible to find the equilibrium points of a system by determining the intersections between the nullclines that represent each specific variable. In this particular case, the equilibrium points of the original system with sigmoid gain function will be determined by the intersection of N_1 and N_2.

$$N_1 \cap N_2 : (a_1 = \tilde{u_1}) \cap (a_2 = \tilde{u_2})$$

Substituting the expressions for u_1 and u_2 that belong to N_1 and N_2 and using the properties associated to the sigmoid function and its inverse gives us the opportunity to conclude that the equilibrium points of this system will satisfy the following equality.

$$\beta\, u_1 + g\, a_2 + F(a_2) = I = \beta\, u_2 + g\, a_1 + F(a_1) \;\Rightarrow\; \beta a_1 + g\, a_2 + F(a_2) = \beta a_2 + g\, a_1 + F(a_1) = I$$

C. XPP codes

C.1 Curtu (2008)'s model

Parameters. Note that the first parameter is, by default, the main bifurcation parameter.

```
    ### Parameters
par I=0, beta=1.1, gamma=0.5
par tau=100
par theta=0.2, k=0.1
gainf(v)=1/(1+exp(-(v-theta)/k))

    ### Equations
u1'=-u1+gainf(-beta*u2-gamma*a1+I)
a1'=(-a1+u1)/tau
u2'=-u2+gainf(-beta*u1-gamma*a2+I)
a2'=(-a2+u2)/tau

    ### Initial conditions
init a1=0.5
init a2=0.5
init u2=0
init u1=1

    ### Integration parameters
@ total=500,meth=rk4,dt=0.01,noutput=2
@ bound=10000,xp=t,yp=u1
@ xlo=-0.1,xhi=300,ylo=-0.1,yhi=1.1
@ xmin=0,xmax=300,ymin=-0.1,ymax=1.1

    ### AUTO parameters
@ autoxmin=0., autoxmax=2, autoymin=-0.2, autoymax=1.2
@ parmin=0,parmax=10.,ds=0.001, dsmax=0.005,dsmin=0.000005
@ Ntst=70
@ Nmax=200, Npr=100

    done
```

C.2 Curtu (2008)'s model with excitatory recurrence

```
### Note that the first parameter is, by default, the main bifurcation parameter.

    ### Parameters
par D=0, beta=0.75, I=0, gamma=0.5
par tau=100
par k=0.1,theta=0.2
gainf(v)=1/(1+exp(-(v-theta)/k))

    ### Equations
u1'=-u1+gainf(D*u1-beta*u2-gamma*a1+I)
a1'=(-a1+u1)/tau
u2'=-u2+gainf(D*u2-beta*u1-gamma*a2+I)
a2'=(-a2+u2)/tau

    ### Initial conditions
init a1=0.5
init a2=0.5
init u2=0
init u1=1

    ### Integration parameters
@ total=500,meth=rk4,dt=0.1,noutput=2
@ bound=10000,xp=t,yp=u1
@ xlo=0,xhi=300,ylo=-0.1,yhi=1.1
@ xmin=0,xmax=300,ymin=-0.1,ymax=1.1

    ### AUTO parameters
@ autoxmin=0., autoxmax=2, autoymin=-0.2, autoymax=1.2
@ Nmax=500, Npr=100, Ntst=50
@ dsmin=0.00001, ds=0.001, dsmax=0.01
@ parmin=-10, parmax=100.

    done
```

C.3 Li et al. (2017)'s attention model

```
### Initial conditions
Rl1(0)=0.9, Rl2(0)=0.1, Rr1(0)=0.2, Rr2(0)=0.8
Hl1(0)=0.8, Hl2(0)=0.1, Hr1(0)=0.1, Hr2(0)=0.2
Rb1(0)=0.9, Rb2(0)=0.9, Hb1(0)=0.3, Hb2(0)=0.2
Ra1(0)=0.6, Ra2(0)=0.5
Ror1(0)=0.3, Ror2(0)=0.7, Rol1(0)=0.1, Rol2(0)=0.7

    ### Parameters
par D=0.0
par wa=0.6
par n1=1
par n2=2
par sigma1=0.2
par sigma2=0.5
par alpha=2
par taus=10
par taua=150
par tauo=20
par tauh=2000
par wo=0.65
par wh=2
par slope=30
par thresh=0.05
hwr(x)=x/(1+exp(-slope*(x-thresh)))    # Half wave rectification function as a smooth function

    # Opponency neurons: Half-wave rectification
Eor1=(hwr(Rr1-Rl1))^n2
Eor2=(hwr(Rr2-Rl2))^n2
Eol1=(hwr(Rl1-Rr1))^n2
Eol2=(hwr(Rl2-Rr2))^n2
Sor=Eor1+Eor2
Sol=Eol1+Eol2
Or=Ror1+Ror2
Ol=Rol1+Rol2

    # Monocular neurons: Half-wave rectification
El1a=hwr(D^n1-wo*Or)
El2a=hwr(D^n1-wo*Or)
Er1a=hwr(D^n1-wo*Ol)
Er2a=hwr(D^n1-wo*Ol)
El1b=hwr(1+wa*Ra1)
El2b=hwr(1+wa*Ra2)
Er1b=hwr(1+wa*Ra1)
Er2b=hwr(1+wa*Ra2)
```

```
El1=El1a*El1b
El2=El2a*El2b
Er1=Er1a*Er1b
Er2=Er2a*Er2b
Sm=El1+El2+Er1+Er2

    # Binocular neurons
Eb1=hwr(Rl1+Rr1)^n2
Eb2=hwr(Rl2+Rr2)^n2
Sb1=Eb1
Sb2=Eb2

    # Attention neurons: Half-wave rectification
Ea1=sign(Rb1-Rb2)*(abs(Rb1-Rb2)^n2)
Ea2=sign(Rb2-Rb1)*(abs(Rb2-Rb1)^n2)
Sa=abs(Ea1)+abs(Ea2)

    ### Equations
# Response binocular neurons (Rb1,Rb2)
Rb1'=(1/taus)*(-Rb1 + Eb1/(Sb1+hwr(Hb1)^n2+sigma2^n2))
Rb2'=(1/taus)*(-Rb2 + Eb2/(Sb2+hwr(Hb2)^n2+sigma2^n2))
Hb1'=(1/tauh)*(-Hb1+wh*Rb1)
Hb2'=(1/tauh)*(-Hb2+wh*Rb2)

    # Response monocular neurons (Rl1,Rl2,Rr1,Rr2)
Rl1'=(1/taus)*(-Rl1+alpha*El1/(Sm+hwr(Hl1)^n1+sigma2^n1))
Rl2'=(1/taus)*(-Rl2+alpha*El2/(Sm+hwr(Hl2)^n1+sigma2^n1))
Rr1'=(1/taus)*(-Rr1+alpha*Er1/(Sm+hwr(Hr1)^n1+sigma2^n1))
Rr2'=(1/taus)*(-Rr2+alpha*Er2/(Sm+hwr(Hr2)^n1+sigma2^n1))
Hl1'=(1/tauh)*(-Hl1+wh*Rl1)
Hl2'=(1/tauh)*(-Hl2+wh*Rl2)
Hr1'=(1/tauh)*(-Hr1+wh*Rr1)
Hr2'=(1/tauh)*(-Hr2+wh*Rr2)

    # Response attention neurons (Ra1,Ra2)
Ra1'=(1/taua)*(-Ra1 + Ea1/(Sa+sigma1^n2))
Ra2'=(1/taua)*(-Ra2 + Ea2/(Sa+sigma1^n2))

    # Response opponency neurons (Ror1,Ror2,Rol1,Rol2)
Ror1'=(1/tauo)*(-Ror1 + Eor1/(Sor+sigma2^n2))
Ror2'=(1/tauo)*(-Ror2 + Eor2/(Sor+sigma2^n2))
Rol1'=(1/tauo)*(-Rol1 + Eol1/(Sol+sigma2^n2))
Rol2'=(1/tauo)*(-Rol2 + Eol2/(Sol+sigma2^n2))
```

```
    ### Integration parameters
@ total=3000,meth=rk4,dt=0.1,noutput=10
@ bound=10000,xp=t,yp=Rb1, yp2=Rb2, nplots=2
@ xlo=0,xhi=300,ylo=-0.1,yhi=1.1
@ xmin=0,xmax=300,ymin=-0.1,ymax=1.1

    ### AUTO parameters
@ autoxmin=0, autoxmax=1.5, autoymin=0, autoymax=1
@ parmin=-10,parmax=100,ds=0.001, dsmax=0.005,dsmin=0.000005
@ Ntst=70
@ Nmax=200, Npr=50

    done
```